Submitted 6 May 2022 to Journal of Physical Oceanography.

A mathematical formalism for circulation in water mass configuration space

A. J. George Nurser[a] Stephen M. Griffies[b] , Jan D. Zika[c,d,e] , and Geoffrey J. Stanley[c]

[a] *National Oceanography Centre, University of Southampton Waterfront Campus, Southampton, UK*
[b] *NOAA Geophysical Fluid Dynamics Laboratory, Princeton, USA &*
Princeton University Program in Atmospheric and Oceanic Sciences, Princeton, USA
[c] *School of Mathematics and Statistics, University of New South Wales, Sydney, Australia*
[d] *UNSW Data Science Hub (uDaSH), University of New South Wales, Sydney, Australia*
[e] *Australian Centre for Excellence in Antarctic Science (ACEAS), University of New South Wales, Sydney, Australia*

ABSTRACT: We present a mathematical formalism for water mass analysis and circulation by formulating mass continuity, tracer continuity, circulation streamfunction, and tracer angular momentum within water mass configuration space ($\boldsymbol{q}$-space), which is defined by an arbitrary number of continuous properties. Points in geometric position space ($\boldsymbol{x}$-space) do not generally correspond in a 1-to-1 manner to points in $\boldsymbol{q}$-space. We therefore formulate $\boldsymbol{q}$-space as a differentiable manifold, which allows for differential and integral calculus but lacks a metric, with the use of exterior algebra and exterior calculus enabling us to develop $\boldsymbol{q}$-space mass and tracer budgets. The Jacobian, which measures the ratio of volumes in $\boldsymbol{x}$-space and $\boldsymbol{q}$-space, is central to our theory. When $\boldsymbol{x}$-space is not 1-to-1 with $\boldsymbol{q}$-space, we define a generalized Jacobian either by patching together $\boldsymbol{x}$-space regions that are 1-to-1 with $\boldsymbol{q}$-space, or by integrating a Dirac delta to select all $\boldsymbol{x}$-space points corresponding to a given $\boldsymbol{q}$ value. The latter method discretizes to a binning algorithm, thus providing a practical framework for water mass analysis. Considering $\boldsymbol{q}$-space defined by tracers, we show that diffusion is directly connected to local tracer space circulation and angular momentum. We also show that diffusion, remarkably, cannot change globally integrated tracer angular momentum (unless different tracers are diffused differently, as in double diffusion), thus leaving only boundary processes (e.g., air-sea or land-sea fluxes), or interior sources to generate globally integrated tracer angular momentum.

1. Introduction

The review paper from Groeskamp et al. (2019) proposed that ocean circulation as described using the kinematics of water mass configuration space (here abbreviated as $\boldsymbol{q}$-space) complements the traditional Eulerian and Lagrangian kinematics (both referred to as $\boldsymbol{x}$-space). We here further this proposition by establishing a mathematical formalism for describing circulation in water mass configuration space. In so doing we expose coordinate-invariant elements of the circulation and reveal novel insights available when choosing specific coordinates. Our goal is not to solve any specific physical problem. Rather, it is to provide a mathematical foundation to support novel views of the ocean circulation.

a. Water mass configuration space

Water mass analysis as introduced by Walin (1977, 1982), and extended by Speer and Tziperman (1992), Nurser et al. (1999), Marshall et al. (1999), Iudicone et al. (2008) (see Groeskamp et al. (2019) for more references), is concerned with seawater motion within and across layers defined by a single tracer concentration or by buoyancy. It therefore involves a 1-D $\boldsymbol{q}$-space, or a mixed 2-D $\boldsymbol{q}$-space using one tracer and one geographical coordinate, commonly latitude ϕ and neutral density $\gamma_{\rm N}$ (Jackett and McDougall 1997), but also temperature and latitude as in Holmes et al. (2019). Isopycnal ocean models are couched in terms of a mixed 3-D $\boldsymbol{q}$-space involving buoyancy, latitude and longitude, while Winters and D'Asaro (1996) used a mixed 3-D $\boldsymbol{q}$-space involving an arbitrary scalar, x and y to study the increased mixing associated with folded and broken-up surfaces of constant scalar. Extension to a 2-D $\boldsymbol{q}$-space involving the two active tracers Conservative Temperature, Θ, and salinity, S, has illuminated our view of the oceanic thermohaline circulation (Speer 1993; Zika et al. 2012; Döös et al. 2012; Hieronymus et al. 2014; Groeskamp et al. 2014), providing images of the ocean circulation such as in Figure 1.

In practice, water mass analysis is concerned with the hows and whys of seawater movement across coordinate surfaces. If those surfaces are defined by tracers or buoyancy, as is traditional, then cross-surface motion is caused by irreversible processes such as mixing, radiant heating, and turbulent boundary fluxes, in which case the associated water mass analysis naturally disregards reversible processes while it focuses on the irreversible. We here further the formalism of water mass analysis with the aim to facilitate the study of ocean circulation within the configuration spaces available from a growing variety of measured ocean properties, such as material tracer concentrations (salinity, carbon, chemical tracers, biogeochemical tracers), dynamical tracers (potential vorticity), thermodynamic properties (Conservative Temperature, pressure), and buoyancy (potential density, neutral density).

Corresponding author: A. J. George Nurser, g.nurser@noc.ac.uk

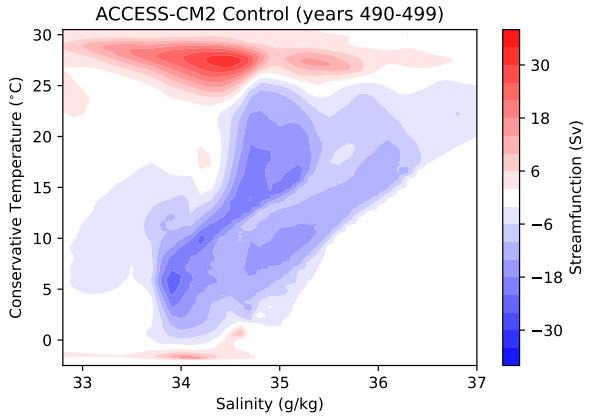

FIG. 1. Global ocean circulation (units of Sv = 10^9 kg s^{-1}) as represented in the water mass configuration space of preformed salinity and Conservative Temperature ($(q^1, q^2) = (S, \Theta)$). The transport is computed from results generated by the ACCESS-CM2 climate model (Bi et al. 2020) run under pre-industrial radiative forcing, and using model years 1440-1449 (years 490-499 of the piControl). Blue (negative) circulation is clockwise and red (positive) is counter-clockwise. See Zika et al. (2012), Döös et al. (2012), Hieronymus et al. (2014), and Groeskamp et al. (2014) for discussions of the physics of this circulation.

Our formulation is partly inspired by the formulation of thermodynamics in Section 5.1 of Schutz (1980) and Section 6.3 of Frankel (2012). Their approach conceives of an equilibrium thermodynamic system as living at a point within a thermodynamic configuration space. Configuration space is generally a smooth and continuous manifold on which the rules of differential and integral calculus hold, and quasi-static processes lead to continuous movement or trajectories on this manifold. Thermodynamic configuration space is not endowed with a metric, but smoothness and continuity ensure it satisfies the properties of a differential manifold (e.g., see chapter 1 of Frankel 2012). The absence of a metric represents a key mathematical distinction from the Euclidean space of Newtonian mechanics, with Euclidean space endowed with the Kronecker metric. Without a metric, we cannot measure distance or angles, and yet we can still derive differential and integral budgets by using rudimentary features of exterior forms (also known as differential forms; see Appendix B). In essence, this paper replaces "thermodynamic configuration space" with "water mass configuration space" and develops the mathematical physics of this space.

We use the language of water mass analysis, being motivated by the many oceanographic applications of circulation in water mass configuration spaces. However, the ocean perspective can be readily extended to the study of atmospheric circulations as viewed in the corresponding "air mass configuration space." The studies from Pauluis and Held (2002), Kjellsson et al. (2014), Laliberté et al. (2015), and Döös et al. (2017) provide examples. Indeed, the formulation given here is fully extendable to any configuration space defined by continuous coordinates.

b. Limitations of water mass configuration space

As in thermodynamics, our formulation is not based on assuming a 1-to-1 invertible relation between $\boldsymbol{q}$-space and $\boldsymbol{x}$-space. Rather, our fundamental assumption is that the chosen water mass coordinates define a water mass configuration space that is a smooth and orientable[1] differential manifold, thus enabling the use of calculus. Starting from this minimalist position allows us to develop a general theory that then offers avenues for specialization.

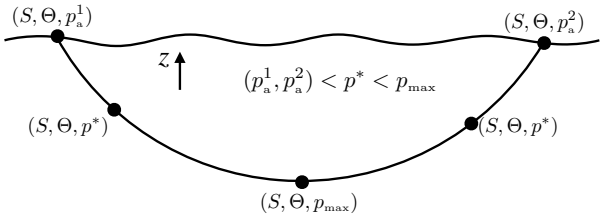

FIG. 2. Illustrating with $\boldsymbol{q} = (S, \Theta, p)$ that the mapping from $\boldsymbol{x}$-space to $\boldsymbol{q}$-space is, generally, not 1-to-1. Here we show a curve of constant (S, Θ), formed by the intersection of a constant S surface and constant Θ surface. This (S, Θ)-curve outcrops at two points on the ocean surface where the atmospheric pressure is p^1_a and p^2_a. Somewhere along the curve there are at least two points with pressure, $p = p^*$, that is less than the maximum pressure along the curve, $p^* < p_{max}$, yet greater than either atmospheric pressures, $(p^1_a, p^2_a) < p^*$. Hence, there are at least two points along the (S, Θ)-curve with the same value for $\boldsymbol{q}$ but distinct values for $\boldsymbol{x}$.

How common is the lack of a global 1-to-1 mapping from $\boldsymbol{x}$-space to $\boldsymbol{q}$-space? The answer depends on specifics of the water mass coordinates. For example, if $\boldsymbol{q}$-space has fewer than three dimensions then there is no continuous function that can map $\boldsymbol{x}$-space 1-to-1 to $\boldsymbol{q}$-space. Even with three water mass coordinates, the lack of 1-to-1 mapping is common. As an illustration, consider the case of thermodynamic coordinates so that $\boldsymbol{q} = (S, \Theta, p)$, as defined by Absolute Salinity, Conservative Temperature, and pressure (Zika et al. 2013). Surfaces of constant Θ and S generally intersect along a curve, with that curve typically outcropping at two distinct points at the sea surface (see Figure 2). For waters deep enough that the pressure is greater than the atmospheric pressure at either of the outcrop points, but shallow enough that the pressure is less than the maximum pressure on this (S, Θ)-curve, there are at least two points in the ocean for each (S, Θ) pair with the same value for (S, Θ, p). So for this rather generic example, the mapping from $\boldsymbol{x}$-space to $\boldsymbol{q}$-space is not globally 1-to-1. As a further example, consider small scale turbulent flows where surfaces of constant property are commonly

[1] A manifold is orientable if we can define handedness continuously over the manifold; i.e., there is a consistent definition of clockwise and counter-clockwise. For example, Euclidean space is orientable whereas a Möbius strip is not.

broken up into discontinuous blobs. For such flows, no global 1-to-1 mapping can be expected.

We pay a price when working within a water mass configuration space that is not afforded a global 1-to-1 mapping from $\boldsymbol{x}$-space. Namely, $\boldsymbol{q}$-space is not generally suited for examining dynamical effects associated with the contact stresses from pressure and friction. The reason is that contact stresses occur between fluid elements that are adjacent in $\boldsymbol{x}$-space, and such locality is lost if the mapping from $\boldsymbol{q}$-space to $\boldsymbol{x}$-space is not 1-to-1. Now there are physically interesting cases where water mass coordinates *do* provide a 1-to-1 mapping from $\boldsymbol{x}$-space, either globally or locally. One example is Salmon (2013), who considered a $\boldsymbol{q}$-space comprised of three tracer-like coordinates that retain a 1-to-1 mapping from $\boldsymbol{x}$-space, and we also consider tracer spaces in this paper (Section 7). Even so, we are not focused on the study of fluid dynamics (i.e., Newton's second or third laws) in $\boldsymbol{q}$-space. Rather, we pursue the traditional approach in water mass analysis by examining ocean circulation in $\boldsymbol{q}$-space as revealed by mass and tracer budgets.

c. *Content of this paper*

We start the main part of this paper in Section 2 by presenting the basic elements of water mass configuration space. We here encounter the central role played by the mass density function, $\mathfrak{m}$, which provides a measure of the seawater mass per unit $\boldsymbol{q}$-space volume. In Section 3 we describe how to relate $\boldsymbol{x}$-space and $\boldsymbol{q}$-space whether or not the mapping between these spaces is 1-to-1. The method we propose allows for a unified treatment of differential budgets derived in subsequent sections. We then provide a $\boldsymbol{q}$-space derivation of mass continuity in Section 4. Although seemingly quite trivial, the resulting continuity equation (55) is fully general and thus provides a measure for mass balances in $\boldsymbol{q}$-space for any number of arbitrary coordinates. We also consider the special case of steady and mass source free circulation, in which we are afforded a $\boldsymbol{q}$-space circulation streamfunction. In Section 5, we introduce the $\boldsymbol{q}$-space angular momentum and derive local and global properties. We find that the $\boldsymbol{q}$-space angular momentum offers a more versatile means to characterize $\boldsymbol{q}$-space circulation than the streamfunction.

In Section 6 we extend the derivation of mass continuity to yield an equation for tracer continuity; i.e., the tracer equation. This discussion is then used in Section 7 whereby we specialize to the study of water mass analysis in tracer space. By allowing tracers to define water mass configuration space, we can connect motion in tracer space to mixing and other irreversible processes. Remarkably, we show that globally integrated properties of the tracer space angular momentum and steady circulation are unaffected by diffusion. We close the main part of the paper in Section 8 with summary and conclusions.

Appendix A provides a few examples for the Laplace operator used for subgrid scale tracer diffusion. In traditional treatments this operator is derived using covariant derivatives, which require a metric tensor. However, our metric-free approach only makes use of partial derivatives. Appendix B rounds out the paper with a tutorial on exterior forms. Both the mathematically experienced reader and the mathematically trusting reader will find Appendix B unnecessary for the main text. Even so, it is offered for the mathematically curious reader who wishes to better understand the mathematical concepts in the main text. Finally, we note that this paper contains many mathematical symbols, with Table 1 summarizing those that are frequently used.

2. Elements of water mass configuration space

We refer to the geographical/depth (position) space as $\boldsymbol{x}$-space and write its corresponding coordinates as

$$\boldsymbol{x} = (x^1, x^2, x^3) = x^a. \tag{1}$$

Labels $a = 1, 2, 3$ distinguish the coordinate components rather than indicate a power. Within a continuum description of seawater, each infinitesimal element of seawater has a unique value for the position coordinate, $\boldsymbol{x}$.

We organize the continuous valued water mass properties into an array

$$\boldsymbol{q} = (q^1, q^2, q^3, \ldots q^N) = q^\alpha, \tag{2}$$

with $N \geq 1$ the number of properties. The properties, q^α, define coordinates for a point within water mass configuration space ($\boldsymbol{q}$-space), with the number of properties, N, determining the dimension of $\boldsymbol{q}$-space. The Greek superscripts signify a particular property rather than denoting a power, and with Greek labels used for $\boldsymbol{q}$-space coordinates as distinguished from the Latin labels used for $\boldsymbol{x}$-space coordinates. Depending on specifics of the water mass coordinates, each point in $\boldsymbol{q}$-space may or may not correspond to a unique point in $\boldsymbol{x}$-space.

a. *Assumptions about $\boldsymbol{q}$-space*

Our mathematical formulation allows for an arbitrary number of water mass coordinates, with examples for $N = 1, 2, 3$ offered in the following to touch base with common applications. Furthermore, $\boldsymbol{q}$-space can be built from any continuous property, including coordinates from $\boldsymbol{x}$-space.

1) $\boldsymbol{q}$-SPACE DEFINES A DIFFERENTIABLE MANIFOLD

We assume that the continuous coordinates of $\boldsymbol{q}$-space define a smooth and orientable differentiable manifold. Doing so allows us to use differential and integral calculus to study mass budgets and circulation in $\boldsymbol{q}$-space. Under these assumptions, water mass configuration space locally

TABLE 1. Table summarizing the key symbols used in this paper.

SYMBOL	MEANING
$\boldsymbol{x}, x^a$	geographical/depth coordinates
a, b, c	$\boldsymbol{x}$-space coordinate labels
$\boldsymbol{q}, q^\alpha$	water mass coordinates with $\alpha \in [1, N]$
N	number of dimensions for $\boldsymbol{q}$-space
α, β, γ	$\boldsymbol{q}$-space coordinate labels
$\dot{\boldsymbol{x}}, \dot{x}^a$	velocity in $\boldsymbol{x}$-space and its components
$\dot{\boldsymbol{q}}, \dot{q}^\alpha$	velocity in $\boldsymbol{q}$-space and its components
$\mathcal{X}$	ocean domain in $\boldsymbol{x}$-space
$\mathfrak{q}$	function measuring $\boldsymbol{q}$ at $\boldsymbol{x} \in \mathcal{X}$
$\dot{\mathfrak{q}}$	function measuring $\dot{\boldsymbol{q}}$ at $\boldsymbol{x} \in \mathcal{X}$
$\mathfrak{q}(\mathcal{X})$	$\boldsymbol{q}$-space image of the ocean domain
$\mathcal{Q}$	subset of $\boldsymbol{q}$-space; codomain of $\mathfrak{q}$
$\partial_a = \partial/\partial x^a$	$\boldsymbol{x}$-space partial derivative
$\partial_\alpha = \partial/\partial q^\alpha$	$\boldsymbol{q}$-space partial derivative
d	exterior derivative operator
$\wedge$	exterior (or wedge) product
$\mathrm{d}V$	$\boldsymbol{x}$-space volume element
$\mathrm{d}\mathcal{V}$	$\boldsymbol{q}$-space volume element
ρ	seawater mass per volume in $\boldsymbol{x}$-space
$\mathfrak{m}$	seawater mass per volume in $\boldsymbol{q}$-space
$\mathrm{d}M$	mass of an elementary ocean region
$\mathcal{J}$	Jacobian from $\boldsymbol{q}$-space to $\boldsymbol{x}$-space
$\mathcal{G}$	inverse Jacobian from $\boldsymbol{x}$-space to $\boldsymbol{q}$-space
$\mathcal{T}$	mass transport exterior form (mass per time)
$\mathcal{M}$	mass source (mass per time)
ψ, ψ_α	steady circulation streamfunctions
$\epsilon^{\alpha\beta} = \epsilon_{\alpha\beta}$	permutation symbol for $\boldsymbol{q}$-space with $N = 2$
$\epsilon^{\alpha\beta\gamma} = \epsilon_{\alpha\beta\gamma}$	permutation symbol for $\boldsymbol{q}$-space with $N = 3$
$\Pi_{\tilde{\boldsymbol{q}}}(\boldsymbol{q})$	Dimensionless boxcar (binning) function
$\delta_{\tilde{\boldsymbol{q}}}(\boldsymbol{q})$	Dirac delta for $\boldsymbol{q}$-space with dimensions $\mathcal{V}^{-1}$
$\delta^\alpha_\beta = \delta_{\alpha\beta}$	Kronecker symbol = unit tensor
$I \in \{1, \ldots, N_{\mathrm{P}}\}$	label for N_{P} coordinate patches
$\boldsymbol{C}, C^\alpha$	tracer concentrations
$\mathcal{T}_C$	tracer transport exterior form
$\rho \boldsymbol{F}, \rho F^a$	$\boldsymbol{x}$-space subgrid tracer flux
$\mathfrak{m} F^\alpha$	$\boldsymbol{q}$-space subgrid tracer flux
$\mathbb{K}$	symmetric diffusivity tensor
$\mathcal{S}$	combined tracer source
S	Absolute Salinity
Θ	Conservative Temperature
p	pressure
ϕ	latitude
γ_{N}	neutral density
$\mathcal{D}$	subgrid tracer operator: $\mathcal{D} = -\mathfrak{m}^{-1} \partial_\alpha (\mathfrak{m} F^\alpha)$

appears like Euclidean space, with differentiation and integration carried from Euclidean space to $\boldsymbol{q}$-space. Hence, differential conservation laws in $\boldsymbol{q}$-space have expressions reminiscent of Cartesian coordinates, and integrals over this manifold take their familiar form. However, there is generally no metric structure in $\boldsymbol{q}$-space. Consequently, we cannot always access familiar tools from vector calculus and tensor analysis, such as distance, angles, outward normal vectors, inner products, covariant derivatives, and curvature.

2) USE OF THE EXTERIOR PRODUCT FOR ORIENTATION

For budget analyses in $\boldsymbol{x}$-space we generally rely on outward normal vectors to orient surfaces, volumes, and transport. However, the absence of a metric for $\boldsymbol{q}$-space affords it a rather minimalist mathematical structure thus necessitating an alternative means for orientation. For that purpose, we orient surfaces and surface elements within $\boldsymbol{q}$-space through the anti-symmetry property of the exterior product, which we introduce in Section 2c and further detail in Appendix B. Doing so allows us to determine whether a transport adds or removes matter from a $\boldsymbol{q}$-space region, thus facilitating the development of budget equations.

3) EMPHASIZING A PROPERTY OF PARTIAL DERIVATIVES

We only make use of partial derivatives throughout this paper, with covariant derivatives not used since they require a metric tensor. When performing partial derivatives, we emphasize that all other coordinates are held fixed. For example, the $\boldsymbol{x}$-space partial derivative,

$$\partial_a = \frac{\partial}{\partial x^a} \tag{3}$$

is computed by holding all coordinates, x^b, fixed, where $b \neq a$. In this manner,

$$\partial_a x^b = \delta^b_a \quad \text{and} \quad \partial_a x^a = 3, \tag{4}$$

with δ^b_a the components to the Kronecker or identity tensor, and the second equality made use of the summation convention where repeated indices are summed over their range. The same identities hold when performing derivatives in $\boldsymbol{q}$-space, so that

$$\partial_\alpha = \frac{\partial}{\partial q^\alpha} \quad \text{and} \quad \partial_\alpha q^\beta = \delta^\beta_\alpha \quad \text{and} \quad \partial_\alpha q^\alpha = N. \tag{5}$$

These identities are central to many of the manipulations in this paper.

b. Mass and mass density in $\boldsymbol{q}$-space

We make use of the mass density function, $\mathfrak{m}(\boldsymbol{q}, t)$, that measures the mass of seawater, $\mathrm{d}M$, within an elemental $\boldsymbol{q}$-space volume, $\mathrm{d}\mathcal{V}$,

$$\mathrm{d}M = \mathfrak{m}\, \mathrm{d}\mathcal{V}. \tag{6}$$

In Figure 3 we illustrate the case of $N = 1$ with $q^1 = \Theta$, so that the ocean is binned according to Conservative Temperature classes. At any time instance, the density function, $\mathfrak{m}(\Theta, t)$, allows us to compute the mass of seawater, $dM = \mathfrak{m}\, d\Theta$, that is contained within a Conservative Temperature bin, $[\Theta - \Delta\Theta/2, \Theta + \Delta\Theta/2)$, in the limit as the bin size becomes infinitesimal, $\Delta\Theta \to d\Theta$. In Figure 4 we extend the configuration space dimension to $N = 2$ by displaying the mass density function for $\boldsymbol{q} = (S, \Theta)$.

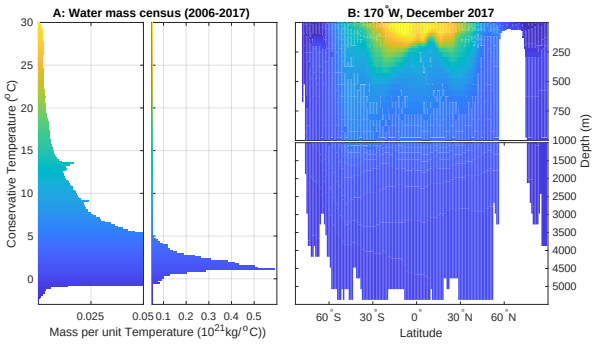

FIG. 3. Left panel (A): mass density function, $\mathfrak{m}(\Theta)$, for a one-dimensional ($N = 1$) water mass configuration space defined by Conservative Temperature, $q^1 = \Theta$, as time averaged over years 2006-2017. The density function has units of 10^{21} kg/°C. Note the split in the horizontal (mass density) axis, thus enabling a more refined view of the density function in the less populated warm and cold waters. Right panel (B): a meridional section at 170°W for December 2017, thus providing a sample of the spatial distribution of Θ. The split in the vertical axis enables a more refined view of the upper ocean warm and cold waters. We use observational based data for the World Ocean as estimated by the objective analysis from the Enact Ensemble (V4.0; Good et al. (2013)).

c. *Volume elements in $\boldsymbol{q}$-space*

The volume element, $d\mathcal{V}$, measures the coordinate volume of an elementary region of $\boldsymbol{q}$-space. For example, with $N = 1$ we have the volume element given by

$$d\mathcal{V} = dq^1, \tag{7}$$

such as the case with $q^1 = \Theta$ discussed above whereby $d\mathcal{V} = d\Theta$. When $N > 1$, we write the volume element as an exterior N-form (N-form for brief)

$$d\mathcal{V} \equiv dq^1 \wedge dq^2 \wedge \ldots dq^N, \tag{8}$$

with $\wedge$ the exterior (or wedge) product. For example, with $N = 3$ and $\boldsymbol{q} = (S, \Theta, p)$, then the volume 3-form in $\boldsymbol{q}$-space is written

$$d\mathcal{V} = dS \wedge d\Theta \wedge dp. \tag{9}$$

Similarly, for $N = 2$ with $\boldsymbol{q} = (S, \Theta)$, the volume 2-form is

$$d\mathcal{V} = dS \wedge d\Theta. \tag{10}$$

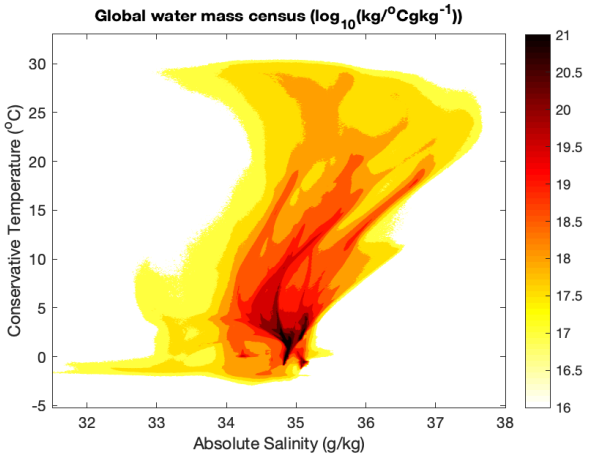

FIG. 4. The log of a mass density function, $\mathfrak{m}(S, \Theta)$ averaged over years 2006-2017 for a two-dimensional ($N = 2$) water mass configuration space defined by Absolute Salinity, S, and Conservative Temperature, Θ, so that $(q^1, q^2) = (S, \Theta)$. The density function has units of kg/[°C (g/kg)]. We use observational based data for the World Ocean as estimated by the objective analysis from the Enact Ensemble (V4.0; Good et al. (2013)). See Zika et al. (2021) for more discussion of this distribution and its changes arising from climate warming.

In Figure 5 we depict the Cartesian area element 2-form $dy \wedge dz$.

The exterior product is anti-symmetric so that odd permutations of differentials lead to a sign change whereas even permutations retain the sign; e.g.,

$$d\mathcal{V} = dS \wedge d\Theta \wedge dp = -d\Theta \wedge dS \wedge dp = dp \wedge dS \wedge d\Theta. \tag{11}$$

Hence, the exterior volume form, $d\mathcal{V}$, is not sign-definite.

3. How to relate $\boldsymbol{x}$-space and $\boldsymbol{q}$-space

In this section we detail how to relate $\boldsymbol{x}$-space and $\boldsymbol{q}$-space. We start in Section 3a by discussing the basic functional properties of the function, $\mathfrak{q}$, that maps from $\boldsymbol{x}$-space to $\boldsymbol{q}$-space. These functional properties split the type of theory for water mass analysis that we can develop into two cases. In Section 3c, we consider the first case, when $N = 3$ and $\mathfrak{q}$ is a bijection between $\boldsymbol{x}$-space and $\boldsymbol{q}$-space. In this case, we can make use of coordinate transformation formulas from elementary calculus and tensor analysis. We review these results and then, in Section 3d, generalize to the second case, where $\mathfrak{q}$ is not a bijection.

a. *Characterizing mappings between $\boldsymbol{x}$-space and $\boldsymbol{q}$-space*

Let $\mathcal{X}$ be a subset of $\boldsymbol{x}$-space that could represent the entire ocean or a subset of the ocean. Note that $\mathcal{X}$ could be time-dependent. Measuring water mass properties at points in the ocean domain, $\boldsymbol{x} \in \mathcal{X}$, and times t determines values for the function $\mathfrak{q}(\boldsymbol{x}, t)$. We assume throughout this paper that $\mathfrak{q}$ is a continuously differentiable function. For

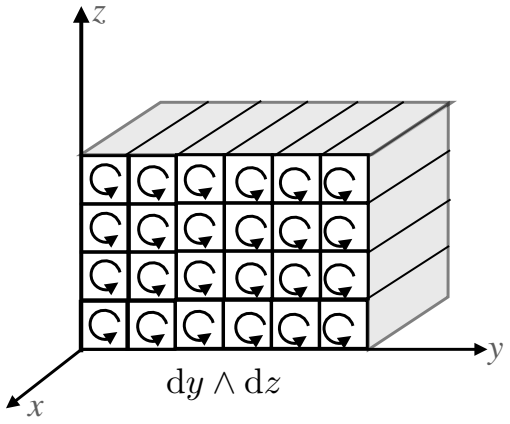

FIG. 5. Schematic of the area 2-form, $\mathrm{d}y \wedge \mathrm{d}z$. For Euclidean space we can establish a geometric interpretation of a 1-form, $\mathrm{d}y$, as an infinite sequence of horizontal planes perpendicular to the y-axis. Likewise, the 1-form, $\mathrm{d}z$, defines surfaces perpendicular to the z-axis. The exterior product, $\mathrm{d}y \wedge \mathrm{d}z$, is the intersection of these surfaces that produces an infinite lattice of infinitesimal oriented cells. By convention, we associate counter-clockwise swirls in each of the infinitesimal cells of area $\mathrm{d}y \wedge \mathrm{d}z$ as a means to orient the area elements according to the right hand rule. This image is adapted from Figure 4.1 of Misner et al. (1973).

brevity, we often treat the time-dependence implicitly; that is, for a fixed time t we simply write $\mathfrak{q}(\boldsymbol{x})$ and treat $\mathfrak{q}$ as a function from domain $\mathcal{X}$ to codomain $\mathcal{Q}$, where $\mathcal{Q}$ is generally a subset of $\boldsymbol{q}$-space. This shorthand applies for the rest of this subsection, in which we restrict attention to a fixed but arbitrary time, t.

In Case 1, let $N = 3$ and suppose that $\mathfrak{q}$ is a *bijection* from $\mathcal{X}$ to $\mathcal{Q}$. This case is equivalent to supposing that $\mathfrak{q}$ is both a *1-to-1* function (also called an *injection*) and an *onto* function (also called a *surjection*). To be 1-to-1 means that $\mathfrak{q}$ maps distinct points in $\mathcal{X}$ to distinct points in $\mathcal{Q}$. That is, if $\boldsymbol{x}_1 \neq \boldsymbol{x}_2$ are two distinct points both in $\mathcal{X}$, then $\mathfrak{q}(\boldsymbol{x}_1) \neq \mathfrak{q}(\boldsymbol{x}_2)$ are two distinct points both in $\mathcal{Q}$. To be onto means that $\mathfrak{q}$ reaches every point in $\mathcal{Q}$; that is, for every $\boldsymbol{q} \in \mathcal{Q}$ there is some $\boldsymbol{x} \in \mathcal{X}$ such that $\mathfrak{q}(\boldsymbol{x}) = \boldsymbol{q}$. Case 1 is depicted in the top panel of Figure 6. As a bijection, the function $\mathfrak{q}$ has an inverse function, denoted $\mathfrak{q}^{-1}$, that is a bijection that maps from $\mathcal{Q}$ to $\mathcal{X}$. As such, no information is lost when using $\mathfrak{q}$ to map between $\mathcal{X}$ and $\mathcal{Q}$.

In Case 2, $\mathfrak{q}$ is not 1-to-1, and may or may not be onto, as depicted in the bottom panel of Figure 6. For $\mathfrak{q}$ to not be 1-to-1 (also called many-to-1) implies that there are distinct points in $\mathcal{X}$ that map to the same point in $\mathcal{Q}$. We introduced the many-to-1 mapping case in Section 1b. Another example in which $\mathfrak{q}$ is many-to-1 occurs if there are finite regions of $\boldsymbol{x}$-space with homogeneous values for some or all of the properties, q^α. Such many-to-1 mappings are not invertible bijections so that information is lost in the process of mapping. While $\mathfrak{q}$ may or may not be many-to-1 for $N \geq 3$, when $N < 3$ it is guaranteed that $\mathfrak{q}$ is many-to-1 (having assumed $\mathfrak{q}$ is continuous). For example, with $\boldsymbol{q} = (\gamma_\mathrm{N}, \phi)$ the zonal direction is integrated out so there is no information about zonal position. Likewise, mapping the ocean to either $\boldsymbol{q} = (S, \Theta)$ or $q = \Theta$ reduces the dimensionality of $\boldsymbol{q}$-space relative to the three dimensions of $\boldsymbol{x}$-space.

The most important distinction between the above two Cases is whether $\mathfrak{q}$ is 1-to-1 or not. If $\mathfrak{q}$ is 1-to-1, we can define the codomain $\mathcal{Q}$ to be the image of $\mathfrak{q}$, denoted $\mathfrak{q}(\mathcal{X})$. While $\mathfrak{q}(\mathcal{X})$ will be time-dependent and may have non-trivial geometric and topological properties, this choice means $\mathfrak{q}$ is onto, by definition, and this further implies that $\mathfrak{q}$ is a bijection, placing us into Case 1 (assuming also that $N = 3$). In Case 2, $\mathfrak{q}$ being many-to-1 implies $\mathfrak{q}$ is not a bijection. Having already lost this desireable property, we care less about whether $\mathfrak{q}$ is onto (surjective).

The upside is that we can define $\mathcal{Q}$ as a larger space than just the set of $\boldsymbol{q}$ values found in the ocean, $\mathfrak{q}(\mathcal{X})$. Most simply, we may define $\mathcal{Q}$ as all of $\boldsymbol{q}$-space, which is the Cartesian product of the valid range for each water mass property q^α. For water mass coordinates that are specified by a material tracer concentration, then the physical value of the coordinate can range between zero and unity, even if the maximum tracer concentration anywhere in the ocean is a small fraction of unity. Similarly, the range for temperature can be extended beyond the values for which seawater is liquid (which depends on pressure and salinity and would thus be time-dependent), to any value above -273.15°C. For example, if $\boldsymbol{q} = (S, \Theta)$ with S measured in g kg^{-1} and Θ in °C, then $\boldsymbol{q}$-space is $[0, 1000] \times [-273.15, \infty)$. We will see that this extension of $\boldsymbol{q}$-space causes no problems, as the functions used in our water mass theory are simply zero outside $\mathfrak{q}(\mathcal{X})$.

In practical calculations of water mass analysis, the mapping $\mathfrak{q}$ from $\boldsymbol{x}$-space to $\boldsymbol{q}$-space is discretely realized via a binning algorithm (e.g., Section 7.5 of Groeskamp et al. (2019)), with the continuous formulation of this paper recovered by letting the bin size be infinitesimal.

b. Trajectories and velocity in $\boldsymbol{x}$-space and $\boldsymbol{q}$-space

We here consider motion in $\boldsymbol{q}$-space and how it is related to motion in $\boldsymbol{x}$-space. Notably, motion in $\boldsymbol{x}$-space may correspond to no motion in $\boldsymbol{q}$-space, for example when $\boldsymbol{q} = (S, \Theta)$ and a fluid element in $\boldsymbol{x}$-space experiences only adiabatic and isohaline physical processes (e.g., linear waves or laminar advection). Likewise, motion in $\boldsymbol{q}$-space could correspond to no motion in $\boldsymbol{x}$-space, for example when $\boldsymbol{q} = (S, \Theta)$ and a region of the ocean is at rest but experiences uniform radiative forcing or uniform diabatic mixing.

The trajectory of a fluid particle in $\boldsymbol{x}$-space, having initial position $\boldsymbol{x}_0$ at time t_0, is described by a function $\boldsymbol{X}(t)$ that satisfies $\boldsymbol{X}(t_0) = \boldsymbol{x}_0$ (e.g., Salmon 1998; van Sebille

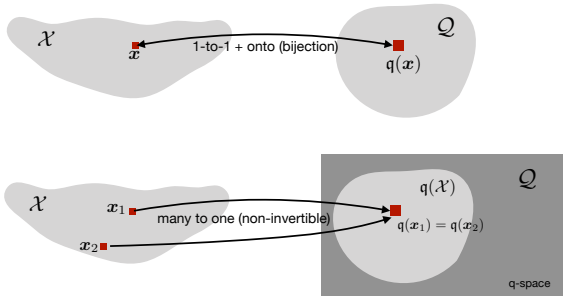

FIG. 6. Two cases for the mapping $\mathfrak{q}$ from $\boldsymbol{x}$-space to $\boldsymbol{q}$-space. The top panel shows Case 1. Here, $\mathfrak{q}$ is 1-to-1: each point in the ocean domain, $\boldsymbol{x} \in \mathcal{X}$, is mapped to a unique point $\mathfrak{q}(\boldsymbol{x})$. Also, $\mathfrak{q}$ is onto: for every point $\boldsymbol{q}$ in the codomain of $\mathfrak{q}$, $\mathcal{Q}$, there is at least one point $\boldsymbol{x} \in \mathcal{X}$ that maps to $\boldsymbol{q}$. Together, these properties imply $\mathfrak{q}$ is a *bijection*, with an inverse function mapping from $\mathcal{Q}$ to $\mathcal{X}$. The bottom panel shows Case 2. Here, $\mathfrak{q}$ is not 1-to-1: two elements from $\boldsymbol{x} \in \mathcal{X}$ are mapped to the same point in $\boldsymbol{q}(\mathcal{X})$. Also, $\mathfrak{q}$ is not onto: the function's image, $\mathfrak{q}(\mathcal{X})$, is a strict subset of the function's codomain, $\mathcal{Q}$. Either of these properties prevents $\mathfrak{q}$ from having a well-defined inverse function from $\mathcal{Q}$ to $\mathcal{X}$. Correspondingly, $\mathfrak{q}$ is not a bijection and information is lost by using $\mathfrak{q}$ to map from $\boldsymbol{x}$-space to $\boldsymbol{q}$-space.

et al. 2018). To determine $\boldsymbol{X}$ requires knowing the velocity, $\dot{\boldsymbol{x}} = \boldsymbol{v}(\boldsymbol{x}, t)$, which in a continuum fluid is a continuous space-time field. Then, $\boldsymbol{X}(t)$ is defined as the integral curve of the velocity field, $\dot{\boldsymbol{x}}$, through the point $(\boldsymbol{x}_0, t_0)$; that is, $\boldsymbol{X}$ solves the ordinary differential equation

$$\frac{\mathrm{d}\boldsymbol{X}(t)}{\mathrm{d}t} = \dot{\boldsymbol{x}}(\boldsymbol{X}(t), t) \quad \text{with} \quad \boldsymbol{X}(t_0) = \boldsymbol{x}_0. \tag{12}$$

Analogously, a trajectory in $\boldsymbol{q}$-space, starting from position $\boldsymbol{q}_0$ at time t_0, is described by a function $\boldsymbol{Q}(t)$ that satisfies $\boldsymbol{Q}(t_0) = \boldsymbol{q}_0$. An example trajectory is depicted in Figure 7. The practical calculation of the trajectory, $\boldsymbol{Q}(t)$, requires knowing the $\boldsymbol{q}$-space velocity, $\dot{\boldsymbol{q}}$, as a field in ($\boldsymbol{q}$-space)-time, i.e. $\dot{\boldsymbol{q}}(\boldsymbol{q}, t)$. Then, $\boldsymbol{Q}$ is defined as the integral curve of the velocity field $\dot{\boldsymbol{q}}$ through the point $(\boldsymbol{q}_0, t_0)$; that is, $\boldsymbol{Q}$ solves the ordinary differential equation

$$\frac{\mathrm{d}\boldsymbol{Q}(t)}{\mathrm{d}t} = \dot{\boldsymbol{q}}(\boldsymbol{Q}(t), t) \quad \text{with} \quad \boldsymbol{Q}(t_0) = \boldsymbol{q}_0. \tag{13}$$

Hence, $\dot{\boldsymbol{q}}$ defines the velocity of a trajectory in $\boldsymbol{q}$-space.

Consider Case 1, in which $\mathfrak{q}$ is a bijection that uniquely maps from $\mathcal{X}$ to $\mathcal{Q}$ at each time instance t. This case enables an interpretation of the $\boldsymbol{q}$-space trajectory, $\boldsymbol{Q}(t)$, through the initial point $\boldsymbol{q}_0 = \boldsymbol{Q}(t_0)$: it is simply the $\boldsymbol{q}$ values along the trajectory $\boldsymbol{X}(t)$ through the initial point $(\boldsymbol{x}_0, t_0)$, where $\boldsymbol{x}_0$ is the unique point in $\mathcal{X}$ that has $\mathfrak{q}(\boldsymbol{x}_0) = \boldsymbol{q}_0$ at time t_0. Mathematically,

$$\boldsymbol{Q}(t) = \mathfrak{q}(\boldsymbol{X}(t), t) \quad \text{with} \quad \mathfrak{q}(\boldsymbol{X}(t_0), t_0) = \boldsymbol{q}_0. \tag{14}$$

Taking the time derivative of equation (14) yields

$$\frac{\mathrm{d}\boldsymbol{Q}(t)}{\mathrm{d}t} = \left[\left.\frac{\partial \mathfrak{q}}{\partial x^a}\right|_{(\boldsymbol{X}(t),t)} \frac{\mathrm{d}X^a(t)}{\mathrm{d}t} + \left.\frac{\partial \mathfrak{q}}{\partial t}\right|_{(\boldsymbol{X}(t),t)} \right] \tag{15a}$$

$$= \dot{\mathfrak{q}}(\boldsymbol{X}(t), t) \tag{15b}$$

$$= \dot{\boldsymbol{q}}(\boldsymbol{Q}(t), t). \tag{15c}$$

In equation (15b), we introduced the function $\dot{\mathfrak{q}}(\boldsymbol{x}, t)$ that measures the $\boldsymbol{q}$-space velocity, $\dot{\boldsymbol{q}}$, at each point in the ocean's $\boldsymbol{x}$-space and time domain. In equation (15c), at a fixed time t, we used the inverse function of $\mathfrak{q}$ to relate $\dot{\boldsymbol{q}}$ at a given $\boldsymbol{q}$ point with $\dot{\mathfrak{q}}$ at the unique $\boldsymbol{x}$ point corresponding to $\boldsymbol{q}$; mathematically,

$$\dot{\boldsymbol{q}}(\boldsymbol{q}) = \dot{\mathfrak{q}}(\mathfrak{q}^{-1}(\boldsymbol{q})). \tag{16}$$

Finally, evaluating equation (14) at $t = t_0$ reveals $\boldsymbol{Q}(t_0) = \boldsymbol{q}_0$, and hence equation (14) satisfies the definition (13).

The interpretation of a $\boldsymbol{q}$-space trajectory as the $\boldsymbol{q}$ values along an $\boldsymbol{x}$-space trajectory (equation (14)) does not generalize to Case 2 when $\mathfrak{q}$ is not a 1-to-1 function. The reason this interpretation fails to generalize is that the fluid particles that had $\boldsymbol{q}$ values of $\boldsymbol{q}_0$ at time t_0 will have an assortment of $\boldsymbol{q}$ values at $t \neq t_0$, and hence differ from the set of fluid particles all having the same $\boldsymbol{q}$ value that we collectively use to define $\dot{\boldsymbol{q}}$ (e.g. equations (34), (39), or (45) ahead).

For either Case 1 or Case 2, $\dot{\boldsymbol{q}}$ corresponds to the dia-surface transport discussed in Section 6.7 of Griffies (2004), Figure 3 of Groeskamp et al. (2014), and Section 2.1 of Groeskamp et al. (2019), thus measuring the transformation of fluid across the respective water mass coordinate surface.

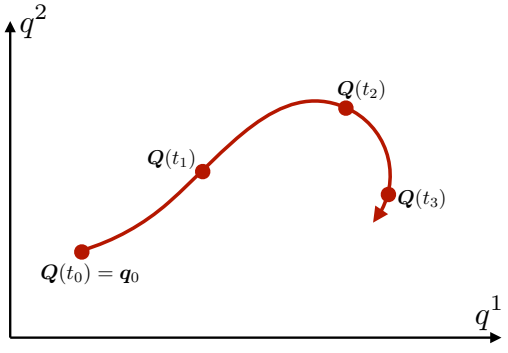

FIG. 7. A sample trajectory, $\boldsymbol{Q}(t)$, in an $N = 2$ dimensional water mass configuration space. We depict positions along the trajectory at four discrete times, with the initial position $\boldsymbol{Q}(t_0) = \boldsymbol{q}_0$.

c. *When $\mathfrak{q}$ is a bijection from $\boldsymbol{x}$-space to $\boldsymbol{q}$-space*

In Case 1, when $N = 3$ and $\mathfrak{q}$ is a bijection (a 1-to-1 and invertible function) from $\mathcal{X}$ to $\mathcal{Q}$, a coordinate transforma-

tion connects mathematical expressions written in $\boldsymbol{x}$-space and $\boldsymbol{q}$-space. The inverse mapping $\mathfrak{x}(\boldsymbol{q}) = \mathfrak{q}^{-1}(\boldsymbol{q})$ gives

$$x^a = x^a(q^1, q^2, q^3) \quad \text{for} \quad a = 1, 2, 3 \tag{17}$$

where $(x^1, x^2, x^3) = (x, y, z)$ are $\boldsymbol{x}$-space Cartesian coordinates. It then follows that the volume element in $\boldsymbol{x}$-space, $\mathrm{d}V$, is related to that in $\boldsymbol{q}$-space through a coordinate transformation realized by the chain rule:

$$\begin{aligned} \mathrm{d}V &= \mathrm{d}x^1 \wedge \mathrm{d}x^2 \wedge \mathrm{d}x^3 && (18a)\\ &= \frac{\partial x^1}{\partial q^\alpha}\,\mathrm{d}q^\alpha \wedge \frac{\partial x^2}{\partial q^\beta}\,\mathrm{d}q^\beta \wedge \frac{\partial x^3}{\partial q^\gamma}\,\mathrm{d}q^\gamma && (18b)\\ &= \mathcal{J}\,\mathrm{d}q^1 \wedge \mathrm{d}q^2 \wedge \mathrm{d}q^3 && (18c)\\ &= \mathcal{J}\,\mathrm{d}\mathcal{V}, && (18d) \end{aligned}$$

where repeated indices are summed over their range. Setting $\mathrm{d}V > 0$ fixes the "standard order" convention for the Cartesian coordinate 1-forms, $\mathrm{d}x^a$. We introduced the Jacobian of the transformation, $\mathcal{J}$, which is the determinant of the transformation matrix from $\boldsymbol{q}$-space to Cartesian coordinates used for $\boldsymbol{x}$-space. The Jacobian is written in the form

$$\mathcal{J} = \det\left(\frac{\partial x^a}{\partial q^\alpha}\right) = \frac{\partial \boldsymbol{x}}{\partial \boldsymbol{q}}, \tag{19}$$

where we introduce the shorthand for the scalar triple product (e.g., Section 1.2 of Salmon (1998))

$$\frac{\partial \boldsymbol{x}}{\partial \boldsymbol{q}} = \left[\frac{\partial \boldsymbol{x}}{\partial q^1} \times \frac{\partial \boldsymbol{x}}{\partial q^2}\right] \cdot \frac{\partial \boldsymbol{x}}{\partial q^3} = \left[\frac{\partial x^1}{\partial \boldsymbol{q}} \times \frac{\partial x^2}{\partial \boldsymbol{q}}\right] \cdot \frac{\partial x^3}{\partial \boldsymbol{q}}, \tag{20}$$

with $\times$ the vector cross product. By the inverse function theorem, $\mathcal{J} \neq 0$ for all $x \in \mathcal{X}$ — under the present assumption that $\mathfrak{q}$ is bijective from $\mathcal{X}$ to $\mathcal{Q}$. Having assumed that $\mathfrak{q}$ is continuously differentiable, then $\mathcal{J}$ is continuous, so $\mathcal{J} \neq 0$ further implies that $\mathcal{J}$ is single-signed. If $\mathcal{J} > 0$ then the coordinate transformation is orientation preserving, whereas $\mathcal{J} < 0$ swaps the orientation.

The Jacobian is central to how we connect physical objects represented in $\boldsymbol{x}$-space to their representation in $\boldsymbol{q}$-space. Geometrically, the Jacobian measures the ratio of the volume elements for the respective coordinates

$$\mathcal{J} = \mathrm{d}V/\mathrm{d}\mathcal{V}, \tag{21}$$

and in so doing it converts between physical dimensions. To illustrate this conversion, consider the mass of an elemental fluid region written in the equivalent manners

$$\mathrm{d}M = \mathfrak{m}\,|\mathrm{d}\mathcal{V}| = \rho\,\mathrm{d}V, \tag{22}$$

with $\rho(\boldsymbol{x}, t)$ the mass per unit volume in $\boldsymbol{x}$-space. The absolute value in equation (22) is needed because $\mathrm{d}M$ and $\mathfrak{m}$ are positive semi-definite but $\mathrm{d}\mathcal{V}$ is not necessarily so. We are thus led to the corresponding relation between the mass per unit volume in $\boldsymbol{x}$-space, $\rho(\boldsymbol{x}, t)$ and the mass density in $\boldsymbol{q}$-space, $\mathfrak{m}$:

$$\mathfrak{m} = \rho\,|\mathcal{J}|, \tag{23}$$

evaluated at an arbitrary $\boldsymbol{q}$. In particular, ρ evaluated at $\boldsymbol{q}$ is just ρ evaluated at the unique point $\boldsymbol{x}$ satisfying $\mathfrak{q}(\boldsymbol{x}) = \boldsymbol{q}$, i.e. $\rho(\boldsymbol{q}) = \rho(\mathfrak{q}^{-1}(\boldsymbol{q}))$, akin to (16). Recall that for an oceanic Boussinesq fluid, mass continuity becomes volume continuity whereby ρ is replaced by a global constant, ρ_0. Even so, the mass density in $\boldsymbol{q}$-space is generally not a constant due to the non-constant Jacobian.

When $\mathfrak{q}$ is a bijection, then $\boldsymbol{q}$-space inherits a full metric structure from $\boldsymbol{x}$-space, and retains the positive definite determinant of the metric tensor. Hence, infinitesimal distances in $\boldsymbol{x}$-space are given in terms of displacements in $\boldsymbol{q}$-space, by

$$(\mathrm{d}s)^2 = (\mathrm{d}\boldsymbol{x} \cdot \mathrm{d}\boldsymbol{x}) = \mathrm{d}q^\alpha g_{\alpha\beta}\,\mathrm{d}q^\beta \tag{24}$$

where

$$g_{\alpha\beta} = \frac{\partial \boldsymbol{x}}{\partial q^\alpha} \cdot \frac{\partial \boldsymbol{x}}{\partial q^\beta} = \frac{\partial x^a}{\partial q^\alpha}\frac{\partial x^a}{\partial q^\beta} \tag{25}$$

is the covariant expression of the metric tensor. It follows that the Jacobian is related to the determinant of $g_{\alpha\beta}$ via

$$|\mathcal{J}| = \sqrt{\det(g_{\alpha\beta})}. \tag{26}$$

d. When the mapping from $\boldsymbol{x}$-space to $\boldsymbol{q}$-space is not 1-to-1

We now consider the more general case when $\mathfrak{q}$ is not a 1-to-1 function from $\mathcal{X}$ to $\mathcal{Q}$. In this case, no global $\mathfrak{x}(\boldsymbol{q}) = \mathfrak{q}^{-1}(\boldsymbol{q})$ exists, and so there is no distance metric or metric tensor. However, it is still possible to define a generalized Jacobian that links the volume elements in $\boldsymbol{q}$-space and $\boldsymbol{x}$-space.

We develop the theory first by patching together results from the previous subsection for regions within which $\mathfrak{q}$ is 1-to-1, and then by summing or integrating over the entire discrete or continuous domain while employing a boxcar or Dirac delta to select only those points in $\boldsymbol{x}$-space with a given $\boldsymbol{q}$ value.

1) Patching regions that are not 1-to-1

To use the theory of Section 3c, we continue with the special case of $N = 3$ for now. The (finite) ocean domain $\mathcal{X}$ can be partitioned into a finite set of regions within each of which $\mathfrak{q}$ is 1-to-1. Now, considering a point $\tilde{\boldsymbol{q}} \in \mathcal{Q}$, there is at most one point $\boldsymbol{x}$ that maps to $\tilde{\boldsymbol{q}}$ in each region. Thus, there are a finite number of points in $\boldsymbol{x}$-space, enumerated $\boldsymbol{x}_I$ for $I = 1, \ldots, N_{\mathrm{P}}$, where $\mathfrak{q}(\boldsymbol{x}_I) = \tilde{\boldsymbol{q}}$. Note that N_{P} depends on $\tilde{\boldsymbol{q}}$. Moreover, assume $\mathcal{G}(\boldsymbol{x}_I) \neq 0$ for each $\boldsymbol{x}_I$, where

$$\mathcal{G}(\tilde{\boldsymbol{x}}) = \left.\frac{\partial \mathfrak{q}}{\partial \boldsymbol{x}}\right|_{\boldsymbol{x}=\tilde{\boldsymbol{x}}} \tag{27}$$

is the inverse Jacobian, i.e. the Jacobian for the mapping $\mathfrak{q}$ from $\boldsymbol{x}$-space to $\boldsymbol{q}$-space. By the inverse function theorem, there exists a small neighborhood, $B(\boldsymbol{x}_I) \subset \mathcal{X}$, with $\boldsymbol{x}_I \in B(\boldsymbol{x}_I)$ and for which the restriction of $\mathfrak{q}$ to $B(\boldsymbol{x}_I)$, denoted $\mathfrak{q}_I : B(\boldsymbol{x}_I) \to \mathfrak{q}(B(\boldsymbol{x}_I))$, is invertible. The inverse of $\mathfrak{q}_I$ satisfies $\mathfrak{q}_I^{-1}(\tilde{\boldsymbol{q}}) = \boldsymbol{x}_I$ and so can be used to evaluate the density at $\tilde{\boldsymbol{q}}$ for the I'th region,

$$\rho_I(\tilde{\boldsymbol{q}}) = \rho(\mathfrak{q}_I^{-1}(\tilde{\boldsymbol{q}})), \tag{28}$$

and likewise the $\boldsymbol{q}$-space velocity at $\tilde{\boldsymbol{q}}$ for the I'th region,

$$\dot{\boldsymbol{q}}_I(\tilde{\boldsymbol{q}}) = \dot{\mathfrak{q}}\big(\mathfrak{q}_I^{-1}(\tilde{\boldsymbol{q}})\big). \tag{29}$$

Similarly, $\mathfrak{q}_I^{-1}$ defines the Jacobian of the mapping from $\boldsymbol{q}$-space to $\boldsymbol{x}$-space at each $\boldsymbol{x}_I$:

$$\mathcal{J}_I(\tilde{\boldsymbol{q}}) = \left.\frac{\partial \mathfrak{x}_I}{\partial \boldsymbol{q}}\right|_{\boldsymbol{q}=\tilde{\boldsymbol{q}}} \quad \text{where} \quad \mathfrak{x}_I(\boldsymbol{q}) = \mathfrak{q}_I^{-1}(\boldsymbol{q}). \tag{30}$$

By the inverse function theorem, $\mathcal{J}_I(\tilde{\boldsymbol{q}}) = 1/\mathcal{G}(\boldsymbol{x}_I)$. Note that the N_P values of $\mathcal{J}_I(\tilde{\boldsymbol{q}})$ need not all have the same sign.

Patching together information about the separate N_P regions, we define the generalized Jacobian at $\tilde{\boldsymbol{q}}$ as the discrete sum of the volume ratios for each region,

$$\mathcal{J}^\text{gen}(\tilde{\boldsymbol{q}}) = \sum_{I=1}^{N_\text{P}} |\mathcal{J}_I(\tilde{\boldsymbol{q}})|. \tag{31}$$

Similarly, the generalized $\boldsymbol{x}$-space mass density at $\tilde{\boldsymbol{q}}$ is

$$\rho^\text{gen}(\tilde{\boldsymbol{q}}) = \frac{1}{\mathcal{J}^\text{gen}(\tilde{\boldsymbol{q}})} \sum_{I=1}^{N_\text{P}} \rho_I(\tilde{\boldsymbol{q}})\,|\mathcal{J}_I(\tilde{\boldsymbol{q}})|, \tag{32}$$

so that the generalized $\boldsymbol{q}$-space mass density at $\tilde{\boldsymbol{q}}$ is

$$\mathfrak{m}^\text{gen}(\tilde{\boldsymbol{q}}) = \rho^\text{gen}(\tilde{\boldsymbol{q}})\,\mathcal{J}^\text{gen}(\tilde{\boldsymbol{q}}) \tag{33a}$$

$$= \sum_{I=1}^{N_\text{P}} \rho_I(\tilde{\boldsymbol{q}})\big|\mathcal{J}_I(\tilde{\boldsymbol{q}})\big|. \tag{33b}$$

Equation (33a) generalizes equation (23) that holds when $\mathfrak{q}$ is bijective. Equation (33b) represents the generalized $\boldsymbol{q}$-space mass density as a discrete sum of the individual $\boldsymbol{q}$-space mass densities for each region, which is analogous to the mass density for a multi-component fluid with N_P components each with mass density $\rho_I|\mathcal{J}_I|$ (e.g., Section 11.11 of Aris (1962)), only here with the components represented by water from different $\boldsymbol{x}$-space patches. In a similar manner, the generalized $\boldsymbol{q}$-space velocity is constructed as a mass-weighted average of the $\boldsymbol{q}$-space velocities from individual regions (each given by equation (16)),

$$\dot{\boldsymbol{q}}^\text{gen}(\tilde{\boldsymbol{q}}) = \frac{1}{\mathfrak{m}^\text{gen}(\tilde{\boldsymbol{q}})} \sum_{I=1}^{N_\text{P}} \dot{\boldsymbol{q}}_I(\tilde{\boldsymbol{q}})\,\rho_I(\tilde{\boldsymbol{q}})\,\big|\mathcal{J}_I(\tilde{\boldsymbol{q}})\big|. \tag{34}$$

At special points where the inverse Jacobian, $\mathcal{G}$, is zero, $\mathcal{J}_I(\tilde{\boldsymbol{q}})$ is infinite and hence so too are $\mathcal{J}^\text{gen}(\tilde{\boldsymbol{q}})$ and $\mathfrak{m}^\text{gen}(\tilde{\boldsymbol{q}})$. We shall say more about this situation soon, but for now we just note that this situation does not indicate a failure of the theory.

Next, we generalize these results to the case in which the dimension N of $\boldsymbol{q}$-space is arbitrary, first with a binning procedure appropriate for discrete data and then for the continuous limit.

2) Generalized transformations with discrete data

Consider a discretized ocean domain, $\mathcal{X}$, that is composed of elementary regions of $\boldsymbol{x}$-space (still denoted $\boldsymbol{x} \in \mathcal{X}$), each with a specified positive volume, $\Delta V(\boldsymbol{x})$. Similarly, consider discretizing $\boldsymbol{q}$-space into bins. Let the bin centered at $\tilde{\boldsymbol{q}}$ be the set $\mathcal{B}(\tilde{\boldsymbol{q}}) \subset \mathcal{Q}$ and have a finite and positive $\boldsymbol{q}$-space volume of $\Delta\mathcal{V}(\tilde{\boldsymbol{q}})$. There may be an arbitrary number of elementary $\boldsymbol{x}$-space regions that map to $\mathcal{B}(\tilde{\boldsymbol{q}})$. At any time instance, we define the generalized Jacobian as the volume ratio of these regions,

$$\mathcal{J}^\text{gen}(\tilde{\boldsymbol{q}}) = \frac{1}{\Delta\mathcal{V}(\tilde{\boldsymbol{q}})} \sum_{\boldsymbol{x}\in\mathcal{X}} \Delta V(\boldsymbol{x})\,\Pi_{\tilde{\boldsymbol{q}}}\big(\mathfrak{q}(\boldsymbol{x})\big), \tag{35}$$

where the sum extends over all points within the discretized ocean, $\boldsymbol{x} \in \mathcal{X}$, and where we introduced the dimensionless boxcar function (e.g., equation (46) of Groeskamp et al. (2019))

$$\Pi_{\tilde{\boldsymbol{q}}}(\boldsymbol{q}) = \begin{cases} 1 & \text{if } \boldsymbol{q} \in \mathcal{B}(\tilde{\boldsymbol{q}}) \\ 0 & \text{otherwise.} \end{cases} \tag{36}$$

Note that $\mathcal{J}^\text{gen}(\tilde{\boldsymbol{q}}) = 0$ if $\mathfrak{q}(\boldsymbol{x}) \notin \mathcal{B}(\tilde{\boldsymbol{q}})$ for all $\boldsymbol{x} \in \mathcal{X}$, i.e. if the bin centered at $\tilde{\boldsymbol{q}}$ is not mapped to by any point in $\boldsymbol{x}$-space.

The generalized $\boldsymbol{x}$-space mass density at $\tilde{\boldsymbol{q}}$ is defined as the mass in all elementary regions $\boldsymbol{x}$ for which $\mathfrak{q}(\boldsymbol{x}) \in \mathcal{B}(\tilde{\boldsymbol{q}})$ divided by the total $\boldsymbol{x}$-space volume of the same regions,

$$\rho^\text{gen}(\tilde{\boldsymbol{q}}) = \frac{\sum_{\boldsymbol{x}\in\mathcal{X}} \rho(\boldsymbol{x})\,\Delta V(\boldsymbol{x})\,\Pi_{\tilde{\boldsymbol{q}}}\big(\mathfrak{q}(\boldsymbol{x})\big)}{\Delta\mathcal{V}(\tilde{\boldsymbol{q}})\;\mathcal{J}^\text{gen}(\tilde{\boldsymbol{q}})}. \tag{37}$$

The definition (37) holds if there is at least one point, $\boldsymbol{x} \in \mathcal{X}$, such that $\mathfrak{q}(\boldsymbol{x}) \in \mathcal{B}(\tilde{\boldsymbol{q}})$, whereas $\rho^\text{gen}(\tilde{\boldsymbol{q}}) = 0$ otherwise. Analogously, the generalized $\boldsymbol{q}$-space mass density at $\tilde{\boldsymbol{q}}$ is the total mass in elementary regions $\boldsymbol{x}$ where $\mathfrak{q}(\boldsymbol{x}) = \tilde{\boldsymbol{q}}$ divided by the $\boldsymbol{q}$-space volume of the bin centered at $\tilde{\boldsymbol{q}}$,

$$\mathfrak{m}^\text{gen}(\tilde{\boldsymbol{q}}) = \frac{1}{\Delta\mathcal{V}(\tilde{\boldsymbol{q}})} \sum_{\boldsymbol{x}\in\mathcal{X}} \rho(\boldsymbol{x})\,\Delta V(\boldsymbol{x})\,\Pi_{\tilde{\boldsymbol{q}}}\big(\mathfrak{q}(\boldsymbol{x})\big) \tag{38a}$$

$$= \rho^\text{gen}(\tilde{\boldsymbol{q}})\;\mathcal{J}^\text{gen}(\tilde{\boldsymbol{q}}). \tag{38b}$$

Like $\mathcal{J}^\text{gen}$, note that $\mathfrak{m}^\text{gen}(\tilde{\boldsymbol{q}}) = 0$ if $\mathfrak{q}(\boldsymbol{x}) \notin \mathcal{B}(\tilde{\boldsymbol{q}})$ for all $\boldsymbol{x} \in \mathcal{X}$. Finally, the generalized $\boldsymbol{q}$-space velocity at $\tilde{\boldsymbol{q}}$ is the mass-weighted average of $\dot{\boldsymbol{q}}$ over regions $\boldsymbol{x} \in \mathcal{X}$ where

$\mathfrak{q}(\boldsymbol{x}) \in \mathcal{B}(\tilde{\boldsymbol{q}})$,

$$\dot{\boldsymbol{q}}^{\text{gen}}(\tilde{\boldsymbol{q}}) = \frac{\sum_{\boldsymbol{x}\in\mathcal{X}} \dot{\mathfrak{q}}(\boldsymbol{x})\,\rho(\boldsymbol{x})\,\Delta V(\boldsymbol{x})\,\Pi_{\tilde{\boldsymbol{q}}}\big(\mathfrak{q}(\boldsymbol{x})\big)}{\Delta\mathcal{V}(\tilde{\boldsymbol{q}})\;\mathfrak{m}^{\text{gen}}(\tilde{\boldsymbol{q}})}. \tag{39}$$

The definition (39) holds if there is at least one point $\boldsymbol{x} \in \mathcal{X}$ with $\mathfrak{q}(\boldsymbol{x}) \in \mathcal{B}(\tilde{\boldsymbol{q}})$, whereas $\dot{\boldsymbol{q}}^{\text{gen}}(\tilde{\boldsymbol{q}}) = 0$ otherwise.

To illuminate the issue raised in Section 3d1 — that the Jacobian $\mathcal{J}$ can be infinite at points where the inverse Jacobian $\mathcal{G}$ is zero — consider an example where $\boldsymbol{q} = \Theta$ and imagine $\Theta = 20°\text{C}$ in the entire ocean. The discretized, generalized Jacobian, $\mathcal{J}^{\text{gen}}$, is zero for each bin except for the one and only bin containing 20°C, where the value of $\mathcal{J}^{\text{gen}}$ is the volume of the entire ocean (in m^3) divided by the volume of this $\boldsymbol{q}$-space bin ($\Delta\mathcal{V} = \Delta\Theta$). As the size of this bin is reduced ($\Delta\Theta \to 0°\text{C}$), the value of $\mathcal{J}^{\text{gen}}$ for the single bin containing 20°C increases towards infinity, but in such a way that $\mathcal{J}^{\text{gen}}\Delta\Theta$ remains finite — namely, the volume of the entire ocean. A similar discussion applies to $\mathfrak{m}^{\text{gen}}$, replacing "volume of the entire ocean" by "mass of the entire ocean". On the other hand, the value of ρ^{gen} in the bin containing 20°C remains finite as the $\boldsymbol{q}$-space bin volume is reduced toward zero: it is the average mass density of the entire ocean. Likewise, $\dot{\boldsymbol{q}}^{\text{gen}}$ also remains finite for the bin containing 20°C: it is the mass-weighted average $\dot{\boldsymbol{q}}$ of the entire ocean. While this discussion illuminates the behavior of these functions as $\Delta\mathcal{V}(\tilde{\boldsymbol{q}}) \to 0$, any individual discretization will have $\Delta\mathcal{V}(\tilde{\boldsymbol{q}}) > 0$, and so the above functions, for the case of discrete data, are finite-valued.

3) Generalized transformations in the continuum

Continuing the case of arbitrary N-dimensional $\boldsymbol{q}$-space, we now consider the continuum limit, wherein the bin sizes are infinitesimal. In this limit, we integrate over $\mathcal{X}$ rather than sum over elementary regions, and the boxcar function is traded for a Dirac delta according to the identity (e.g. Appendix II of Cohen-Tannoudji et al. 1977)

$$\delta_{\tilde{\boldsymbol{q}}}(\boldsymbol{q}) = \lim_{\Delta\mathcal{V}(\tilde{\boldsymbol{q}})\to 0} \frac{\Pi_{\tilde{\boldsymbol{q}}}(\boldsymbol{q})}{\Delta\mathcal{V}(\tilde{\boldsymbol{q}})}. \tag{40}$$

The Dirac delta, $\delta_{\tilde{\boldsymbol{q}}}$, carries dimensions of $\mathcal{V}^{-1}$ and is marked to a specific point $\tilde{\boldsymbol{q}}$ (rather than to the origin, as the manifold $\mathcal{Q}$ lacks the notion of an origin). Multiplying equation (40) by a smooth function, $f(\boldsymbol{q})$, and integrating over $\mathcal{Q}$ reveals that $\delta_{\tilde{\boldsymbol{q}}}$ satisfies the sifting property,

$$\int_{\mathcal{Q}} f(\boldsymbol{q})\delta_{\tilde{\boldsymbol{q}}}(\boldsymbol{q})\,\mathrm{d}\mathcal{V} = \begin{cases} f(\tilde{\boldsymbol{q}}) & \text{if } \tilde{\boldsymbol{q}} \in \mathcal{Q} \\ 0 & \text{if } \tilde{\boldsymbol{q}} \notin \mathcal{Q}. \end{cases} \tag{41}$$

Choosing $f(\boldsymbol{q}) = 1$ reveals how $\delta_{\tilde{\boldsymbol{q}}}$ is normalized, integrating to 1 if $\tilde{\boldsymbol{q}} \in \mathcal{Q}$, otherwise integrating to 0.

In the continuum limit, the generalized Jacobian from equation (35) becomes

$$\mathcal{J}^{\text{gen}}(\tilde{\boldsymbol{q}}) = \int_{\mathcal{X}} \delta_{\tilde{\boldsymbol{q}}}\big(\mathfrak{q}(\boldsymbol{x})\big)\,\mathrm{d}V. \tag{42}$$

Note that $\mathcal{J}^{\text{gen}}(\tilde{\boldsymbol{q}}) = 0$ if $\tilde{\boldsymbol{q}} \notin \mathfrak{q}(\mathcal{X})$ — that is, if $\tilde{\boldsymbol{q}}$ is not mapped to by any point $\boldsymbol{x} \in \mathcal{X}$. Similarly, for all points $\tilde{\boldsymbol{q}} \in \mathfrak{q}(\mathcal{X})$, the generalized $\boldsymbol{x}$-space mass density at $\tilde{\boldsymbol{q}}$ from equation (37), the generalized $\boldsymbol{q}$-space mass density from equation (38b), and the generalized $\boldsymbol{q}$-space velocity from equation (39), each become

$$\rho^{\text{gen}}(\tilde{\boldsymbol{q}}) = \frac{1}{\mathcal{J}^{\text{gen}}(\tilde{\boldsymbol{q}})} \int_{\mathcal{X}} \rho(\boldsymbol{x})\,\delta_{\tilde{\boldsymbol{q}}}\big(\mathfrak{q}(\boldsymbol{x})\big)\,\mathrm{d}V, \tag{43}$$

$$\mathfrak{m}^{\text{gen}}(\tilde{\boldsymbol{q}}) = \int_{\mathcal{X}} \rho(\boldsymbol{x})\,\delta_{\tilde{\boldsymbol{q}}}\big(\mathfrak{q}(\boldsymbol{x})\big)\,\mathrm{d}V \tag{44a}$$

$$= \rho^{\text{gen}}(\tilde{\boldsymbol{q}})\,\mathcal{J}^{\text{gen}}(\tilde{\boldsymbol{q}}), \tag{44b}$$

$$\dot{\boldsymbol{q}}^{\text{gen}}(\tilde{\boldsymbol{q}}) = \frac{1}{\mathfrak{m}^{\text{gen}}(\tilde{\boldsymbol{q}})} \int_{\mathcal{X}} \dot{\mathfrak{q}}(\boldsymbol{x})\,\rho(\boldsymbol{x})\,\delta_{\tilde{\boldsymbol{q}}}\big(\mathfrak{q}(\boldsymbol{x})\big)\,\mathrm{d}V. \tag{45}$$

If $\tilde{\boldsymbol{q}} \notin \mathfrak{q}(\mathcal{X})$, then $\rho^{\text{gen}}(\tilde{\boldsymbol{q}}) = 0$, $\mathfrak{m}^{\text{gen}}(\tilde{\boldsymbol{q}}) = 0$, and $\dot{\boldsymbol{q}}^{\text{gen}}(\tilde{\boldsymbol{q}}) = 0$.

If $\tilde{\boldsymbol{q}} = \mathfrak{q}(\boldsymbol{x})$ for some $\boldsymbol{x}$ at which $\mathcal{G}(\boldsymbol{x}) = 0$, then $\mathcal{J}^{\text{gen}}(\tilde{\boldsymbol{q}})$ is, loosely speaking, infinite. (This singular behavior arises via the composition of the Dirac delta with $\mathfrak{q}(\boldsymbol{x})$ in equation (42), which can be re-expressed as the Dirac delta divided by $|\mathcal{G}|$.) However, this singularity is controlled, in that the integral of $\mathcal{J}^{\text{gen}}$ over a region of $\boldsymbol{q}$-space remains finite. This situation is analogous to how the integral of the Dirac delta $\delta_{\tilde{\boldsymbol{q}}}$ is finite, despite $\delta_{\tilde{\boldsymbol{q}}}$ being "infinite" at $\tilde{\boldsymbol{q}}$. Mathematically, $\mathcal{J}^{\text{gen}}$ is, like $\delta_{\tilde{\boldsymbol{q}}}$, a *distribution* or a *generalized function* rather than a function in the ordinary sense (e.g., see Chapters 1 and 5 in Stakgold (2000a,b)). Returning to the example of $\boldsymbol{q} = \Theta$ and an ocean of uniform $\Theta = 20°\text{C}$ but now in the continuum case, what matters is that $\int_a^b \mathcal{J}^{\text{gen}}(\Theta)\,\mathrm{d}\Theta$ returns the volume of the entire ocean if $20°\text{C} \in [a, b]$ and returns 0 otherwise.

4) Notation convention

In the following, we make use of the more succinct notation from Section 3c, effectively dropping the "gen" superscripts. Yet when $\mathfrak{q}$ is not a bijection, we assume the formalism of the present subsection (either the discrete or continuum case as appropriate) has been used to compute the generalized Jacobian, generalized mass density, and generalized $\boldsymbol{q}$-space velocity. In so doing, the formulation in the following sections is appropriate whether $\mathfrak{q}$ is bijective or not.

e. Boundaries in $\boldsymbol{q}$-space

Boundaries in $\boldsymbol{x}$-space are specified by the geometry of the domain, $\mathcal{X}$, containing the fluid; i.e., by the ocean bottom and ocean surface. If, at each time t, the function $\mathfrak{q}$ is bijective from $\mathcal{X}$ to $\mathcal{Q}$ (Case 1), then boundaries of $\mathcal{X}$ correspond to boundaries of $\mathcal{Q}$. However, in the absence of a 1-to-1 mapping from $\mathcal{X}$ to $\mathcal{Q}$ (Case 2), water mass space has no direct information about the ocean geometry. Hence, boundaries in $\boldsymbol{q}$-space require distinct considerations from those in $\boldsymbol{x}$-space.

With our choice for Case 2 that $\mathcal{Q}$ is all of $\boldsymbol{q}$-space (Section 3a), the boundaries of $\mathcal{X}$ correspond to points in the interior of $\mathcal{Q}$. As such, $\boldsymbol{x}$-space boundary fluxes must appear as source terms in $\boldsymbol{q}$-space. For example, a mass flux (e.g., evaporation, precipitation) that crosses the boundary of the ocean domain, $\partial\mathcal{X}$, must be handled as a source in $\boldsymbol{q}$-space for that $\boldsymbol{q}$-space point where the mass enters. Likewise, for tracers used to define $\boldsymbol{q}$-space coordinates, the $\boldsymbol{x}$-space boundary tracer flux must appear as a corresponding $\boldsymbol{q}$-space source.

4. Mass continuity

There have been two approaches to working with water mass configuration space. In the treatments of Marshall et al. (1999), Iudicone et al. (2008) and Groeskamp et al. (2019), the integration and differentiation are performed in $\boldsymbol{x}$-space and the results transformed to $\boldsymbol{q}$-space. In contrast, in the treatment of Walin (1977) and, for example, Nurser et al. (1999), volume elements, diabatic forcing, fluxes, and other quantities are first projected onto $\boldsymbol{q}$-space and the budgets also performed in $\boldsymbol{q}$-space. We here follow the $\boldsymbol{q}$-space approach, offering further rigor to the method and extending it to $\boldsymbol{q}$-space with arbitrary dimension, N.

a. Mass transport exterior form

We here make use of exterior forms (Appendix B) since they do not rely on a metric structure. To derive the mass budget for a region fixed in $\boldsymbol{q}$-space, we introduce the mass transport exterior form that measures the oriented mass transport through an N-1 dimensional surface. The formalism holds for an arbitrary number of $\boldsymbol{q}$-space dimensions, and we display results for $N = 1, 2, 3$.

Starting with $N = 3$ we introduce the mass transport 2-form

$$\mathcal{T} = \mathfrak{m}\,(\dot{q}^1\,\mathrm{d}q^2 \wedge \mathrm{d}q^3 + \dot{q}^2\,\mathrm{d}q^3 \wedge \mathrm{d}q^1 + \dot{q}^3\,\mathrm{d}q^1 \wedge \mathrm{d}q^2), \quad (46)$$

with $\mathcal{T}$ having dimensions of mass per time. Following Section 2.9b of Frankel (2012), we mathematically interpret $\mathcal{T}$ as the interior product (see also Appendix B3) of the vector $\mathfrak{m}\,\dot{\boldsymbol{q}}$ with the volume N-form $\mathrm{d}\mathcal{V}$. Thus equation (46) follows from equations (B9) and (B10). Physically, we interpret $\mathfrak{m}\,\dot{q}^1\,\mathrm{d}q^2 \wedge \mathrm{d}q^3$ as the mass transport (mass per time) penetrating the infinitesimal surface element in $\boldsymbol{q}$-space defined by $\mathrm{d}q^2 \wedge \mathrm{d}q^3$. We take the right hand convention so that a positive $\dot{q}^1$ leads to mass transport from the negative side to the positive side of the infinitesimal surface defined by $\mathrm{d}q^2$ and $\mathrm{d}q^3$. Analogous interpretations hold for the other two terms. Also, recall the geometric interpretation in Figure 5 for the area element 2-form for the special case of Cartesian coordinates.

For $N = 2$, the interior product equation (B9) gives the mass transport 1-form as

$$\mathcal{T} = \mathfrak{m}\,\epsilon_{\alpha\beta}\dot{q}^\alpha\,\mathrm{d}q^\beta = \mathfrak{m}\,(\dot{q}^1\,\mathrm{d}q^2 - \dot{q}^2\,\mathrm{d}q^1), \quad (47)$$

where we used $\epsilon_{12} = -\epsilon_{21} = 1$ and $\epsilon_{11} = \epsilon_{22} = 0$. For example, with $(q^1, q^2) = (S, \Theta)$, the water mass transport 1-form is given by

$$\mathcal{T} = \mathfrak{m}\,(\dot{S}\,\mathrm{d}\Theta - \dot{\Theta}\,\mathrm{d}S). \quad (48)$$

With $N = 1$ we make use of the mass transport 0-form given by

$$\mathcal{T} = \mathfrak{m}\,\dot{q}. \quad (49)$$

In this case, flow occurs along the single coordinate direction. For example, when binning the ocean according to temperature, then $\mathcal{T} = \mathfrak{m}\,\dot{\Theta}$.

b. Deriving the mass continuity equation

We here develop the mass continuity equation, which is the continuum budget for mass contained in an infinitesimal elemental region fixed in $\boldsymbol{q}$-space. That is, we want to determine what affects the time derivative

$$\partial_t\,(\mathrm{d}M) = \partial_t\,(\mathfrak{m}\,\mathrm{d}\mathcal{V}) = (\partial_t\mathfrak{m})\,\mathrm{d}\mathcal{V}, \quad (50)$$

where the time derivative is computed holding the $\boldsymbol{q}$-coordinates fixed so that $\partial_t\,(\mathrm{d}\mathcal{V}) = 0$.

Just as when developing the Eulerian mass budget for $\boldsymbol{x}$-space, we presume that the mass of an elemental region of $\boldsymbol{q}$-space is affected by the accumulation of mass transported into the volume of $\boldsymbol{q}$-space, along with any mass sources. These considerations lead us to formulate the mass budget for an elemental volume in $\boldsymbol{q}$-space in the generic manner

$$(\partial_t\mathfrak{m})\,\mathrm{d}\mathcal{V} = -\mathrm{d}\mathcal{T} + \mathcal{M}\,\mathrm{d}\mathcal{V} \quad (51)$$

with the $\boldsymbol{q}$-space mass source (mass per time) given by $\mathcal{M}\,\mathrm{d}\mathcal{V}$, and with $\mathrm{d}\mathcal{T}$ the spatial exterior derivative of the mass transport exterior form.

We derive a more conventional form of the mass continuity equation (51) by considering the case of $N = 2$, in which the spatial exterior derivative of the transport 1-form

is given by (see Appendix B4 for details)

$$\begin{aligned} \mathrm{d}\mathcal{T} &= \mathrm{d}\left[\mathfrak{m}\,\dot{q}^1\,\mathrm{d}q^2 - \mathfrak{m}\,\dot{q}^2\,\mathrm{d}q^1\right] && (52a)\\ &= \partial_{q^1}(\mathfrak{m}\,\dot{q}^1)\,\mathrm{d}q^1\wedge\mathrm{d}q^2 - \partial_{q^2}(\mathfrak{m}\,\dot{q}^2)\,\mathrm{d}q^2\wedge\mathrm{d}q^1 && (52b)\\ &= [\partial_{q^1}(\mathfrak{m}\,\dot{q}^1) + \partial_{q^2}(\mathfrak{m}\,\dot{q}^2)]\,\mathrm{d}q^1\wedge\mathrm{d}q^2 && (52c)\\ &= [\partial_{q^1}(\mathfrak{m}\,\dot{q}^1) + \partial_{q^2}(\mathfrak{m}\,\dot{q}^2)]\,\mathrm{d}\mathcal{V}. && (52d) \end{aligned}$$

In the above we noted that anti-symmetry of the exterior product means that

$$\mathrm{d}q^1\wedge\mathrm{d}q^1 = \mathrm{d}q^2\wedge\mathrm{d}q^2 = 0. \tag{53}$$

Furthermore, we used the property of the exterior derivative, whereby it is an anti-symmetrized derivative operator so that the exterior derivative of a p-form produces a $(p+1)$-form. Using $\mathrm{d}\mathcal{T}$ in the form of equation (52d) in the mass continuity equation (51), and then cancelling the common $\mathrm{d}\mathcal{V}$ factor, leads to the $\boldsymbol{q}$-space mass continuity equation

$$\partial_t\mathfrak{m} = -\partial_{q^1}(\mathfrak{m}\,\dot{q}^1) - \partial_{q^2}(\mathfrak{m}\,\dot{q}^2) + \mathcal{M}. \tag{54}$$

This result readily generalizes to arbitrary dimensions of $\boldsymbol{q}$-space

$$\partial_t\mathfrak{m} = -\partial_\alpha(\mathfrak{m}\,\dot{q}^\alpha) + \mathcal{M} = -\nabla_{\boldsymbol{q}}\cdot(\mathfrak{m}\,\dot{\boldsymbol{q}}) + \mathcal{M}. \tag{55}$$

The second equality introduced the operator, $\nabla_{\boldsymbol{q}}$, as a shorthand for the water mass partial derivative operators. The flux-form continuity equation (55) can be written in the equivalent advective form by expanding the $\partial/\partial q^\alpha$ derivatives

$$(\partial_t + \dot{q}^\alpha\,\partial_\alpha)\,\mathfrak{m} = -\mathfrak{m}\,\partial_\alpha\dot{q}^\alpha + \mathcal{M}. \tag{56}$$

The mass continuity equation (55) reveals that the $\boldsymbol{q}$-space mass density, $\mathfrak{m}$, changes in time within a fixed $\boldsymbol{q}$-space elemental region according to mass sources as well as the $\boldsymbol{q}$-space convergence of the mass flux. It is the natural, seemingly trivial, generalization of the Cartesian coordinate continuity equation. However, we emphasize that the derivation made no use of $\boldsymbol{x}$-space nor any metric structure. Furthermore, the differential operators are partial derivatives rather than covariant derivatives.

c. Example coordinates

We consider examples of the mass continuity equation (55) to help garner some confidence in its use. First, we trivially recover the Cartesian $\boldsymbol{x}$-space continuity equation by setting $\boldsymbol{q} = \boldsymbol{x}$, $\mathfrak{m} = \rho$, and $\mathcal{M} = 0$ so that

$$\partial_t\rho = -\partial_x(\rho\,\dot{x}) - \partial_y(\rho\,\dot{y}) - \partial_z(\rho\,\dot{z}) = -\nabla\cdot(\rho\,\boldsymbol{v}), \tag{57}$$

with $\boldsymbol{v} = \dot{\boldsymbol{x}}$ the velocity of a fluid particle in $\boldsymbol{x}$-space.

Consider next the case of generalized vertical coordinates as introduced by Starr (1945) and used in many ocean models (e.g., Griffies et al. 2020). In this case, $\boldsymbol{q} = (x, y, \sigma)$, where $\sigma = \sigma(x, y, z, t)$ is a vertical coordinate such as the hydrostatic pressure, potential density, or a variety of hybrid options. It is common to insist that all generalized vertical coordinates satisfy the constraint that the Jacobian of transformation between $\boldsymbol{x}$-space and generalized vertical coordinates,

$$\mathcal{J} = \frac{\partial z}{\partial\sigma}, \tag{58}$$

also known as the specific thickness, is strictly non-zero and single-signed. This assumption ensures that there is a 1-to-1 and invertible relation between σ and z for any (x, y, t). In this case the continuity equation is

$$\partial_t\mathfrak{m} = -\partial_x(\mathfrak{m}\,\dot{x}) - \partial_y(\mathfrak{m}\,\dot{y}) - \partial_\sigma(\mathfrak{m}\,\dot{\sigma}), \tag{59}$$

with the mass density given by

$$\mathfrak{m} = \rho\,|\mathcal{J}| = \rho\left|\frac{\partial z}{\partial\sigma}\right|. \tag{60}$$

For a Boussinesq ocean, ρ is set to a constant reference value within the mass and tracer continuity equations, in which case the continuity equation (59) becomes an equation for the specific thickness (e.g., equation (37) in Young (2012))

$$\partial_t\mathcal{J} = -\partial_x(\mathcal{J}\,\dot{x}) - \partial_y(\mathcal{J}\,\dot{y}) - \partial_\sigma(\mathcal{J}\,\dot{\sigma}). \tag{61}$$

Now consider $\boldsymbol{q} = (S, \Theta, p)$, again assuming the function $\mathfrak{q}$ from $\mathcal{Q}$ to $\mathcal{X}$ is bijective. The Jacobian determinant is given by

$$\mathcal{J} = \left[\frac{\partial\boldsymbol{x}}{\partial S}\times\frac{\partial\boldsymbol{x}}{\partial\Theta}\right]\cdot\frac{\partial\boldsymbol{x}}{\partial p}, \tag{62}$$

so that the mass density, $\mathfrak{m} = \rho\,|\mathcal{J}|$, is stretched and squeezed according to the distribution of the seawater volume within (S, Θ, p)-space. Accordingly, the continuity equation is

$$\partial_t\mathfrak{m} = -\partial_S(\mathfrak{m}\,\dot{S}) - \partial_\Theta(\mathfrak{m}\,\dot{\Theta}) - \partial_p(\mathfrak{m}\,\dot{p}) + \mathcal{M}. \tag{63}$$

Notably, this form of the continuity equation holds even if the function $\mathfrak{q}$ from $\mathcal{X}$ to $\mathcal{Q}$ is not bijective, since we can use the generalized mass density (44) and $\boldsymbol{q}$-space linear momentum (45).

For the two dimensional water mass configuration space, $\boldsymbol{q} = (S, \Theta)$,

$$\partial_t\mathfrak{m} = -\partial_S(\mathfrak{m}\,\dot{S}) - \partial_\Theta(\mathfrak{m}\,\dot{\Theta}) + \mathcal{M} \tag{64}$$

Here, the function $\mathfrak{q}$ cannot be 1-to-1 from the 2D $\boldsymbol{q}$-space and 3D $\boldsymbol{x}$-space, so we must always use the generalized mass density (44) and $\boldsymbol{q}$-space linear momentum (45). We can integrate the mass continuity equation (64) over a finite

region of $\boldsymbol{q}$-space to develop finite volume budgets. Flow from relatively fresh to salty, $\mathfrak{m}\dot{S} > 0$, arises from salt inputs, while flows from relatively cold to warmer, $\mathfrak{m}\dot{\Theta} > 0$, are driven by heat input. The convergence of the mass transports renders a time change to the mass density, $\mathfrak{m}$, and hence the mass contained in each cell. In this manner, the mass budget of the volume in $\boldsymbol{x}$-space enclosed by surfaces of constant S and Θ, that are generally quite complex, is simplified into the mass budget of grid cells in $\boldsymbol{q}$-space.

d. Steady circulation in $\boldsymbol{q}$-space

In the absence of $\boldsymbol{q}$-space mass sources ($\mathcal{M} = 0$) and for a steady state, the continuity equation (51) says that the mass transport exterior form has zero spatial exterior derivative

$$\mathrm{d}\mathcal{T} = 0, \tag{65}$$

in which case we say that $\mathcal{T}$ is a spatially closed exterior form. If water mass space is both simply connected (i.e., we can continuously shrink any simple closed curve into a point while remaining in the domain) and orientable, then $\mathcal{T}$ is both closed and exact. In this case, and with $N > 1$, we can introduce a globally defined streamfunction, ψ, that satisfies

$$\mathcal{T} = \mathrm{d}\psi, \tag{66}$$

with $\mathrm{d}^2\psi = 0$ equivalent to the vanishing divergence of a curl (see Appendix B4).

The steady and source free mass continuity equation (55) leads to the $\boldsymbol{q}$-space non-divergence condition for the $\boldsymbol{q}$-space mass flux

$$\nabla_{\boldsymbol{q}} \cdot (\mathfrak{m}\,\dot{\boldsymbol{q}}) = \partial_\alpha(\mathfrak{m}\,\dot{q}^\alpha) = 0. \tag{67}$$

For $N = 1$, $\mathcal{T} = \mathfrak{m}\,\dot{q}^1$, which is a 0-form (i.e., a function) that is constant, and thus a special case. For $N = 2$, the streamfunction is a 0-form (i.e., a function) defined on the $N = 2$ dimensional $\boldsymbol{q}$-space domain, $\psi(q^1, q^2)$. Its exterior derivative is

$$\mathrm{d}\psi = \partial_\alpha\psi\,\mathrm{d}q^\alpha = \mathcal{T} = \mathfrak{m}\,(\dot{q}^1\,\mathrm{d}q^2 - \dot{q}^2\,\mathrm{d}q^1), \tag{68}$$

so that

$$\mathfrak{m}\,\dot{q}^\alpha = \epsilon^{\alpha\beta}\,\partial_\beta\psi, \tag{69}$$

with $\epsilon^{\alpha\beta}$ the totally anti-symmetric permutation symbol for $N = 2$, and with ψ having physical dimensions of mass per time, M/T. For $N = 3$, where the mass transport 2-form is given by equation (46), the streamfunction is a 1-form defined on the $N = 3$ dimensional $\boldsymbol{q}$-space domain, in which

$$\mathcal{T} = \mathrm{d}(\psi_\alpha\,\mathrm{d}q^\alpha). \tag{70}$$

Following the steps in Appendix B4d for taking the exterior derivative of a 1-form leads to

$$\mathfrak{m}\,\dot{q}^\alpha = \epsilon^{\alpha\beta\gamma}\,\partial_\beta\psi_\gamma, \tag{71}$$

with $\epsilon^{\alpha\beta\gamma}$ the totally anti-symmetric permutation symbol for $N = 3$, and with the streamfunction components, ψ_γ, having physical dimensions of $\mathrm{M}/(\mathrm{T}\,q^\gamma)$.

5. Water mass angular momentum

We here introduce the water mass angular momentum as a measure of circulation in $\boldsymbol{q}$-space for dimensions $N > 1$. The use of angular momentum does not rely on the steady and source-free assumption required for the streamfunction of Section 4d. For a $\boldsymbol{q}$-space of dimension $N = 2$ and $N = 3$, we define the angular momenta

$$N = 2: \quad L = \epsilon_{\beta\gamma}\,q^\beta\,\dot{q}^\gamma\,\mathfrak{m}\,\mathrm{d}\mathcal{V} \tag{72a}$$

$$N = 3: \quad L_\alpha = \epsilon_{\alpha\beta\gamma}\,q^\beta\,\dot{q}^\gamma\,\mathfrak{m}\,\mathrm{d}\mathcal{V}, \tag{72b}$$

where $\epsilon_{\beta\gamma}$ and $\epsilon_{\alpha\beta\gamma}$ are permutation symbols that are numerically identical to those written with raised indices in equations (69) and (71). Water mass angular momentum for higher dimensional $\boldsymbol{q}$-spaces can be defined by adding an index to the permutation symbol. Conversely, water mass angular momentum for $N = 1$ is not defined since motion with $N = 1$ occurs only along the single coordinate axis.

a. Examples and basic properties

For the case when $\boldsymbol{q} = \boldsymbol{x}$ with $N = 3$ we recover the angular momentum from Cartesian fluid mechanics

$$\boldsymbol{L} = \boldsymbol{x} \times \boldsymbol{p}, \tag{73}$$

where $\boldsymbol{p} = \dot{\boldsymbol{x}}\,\rho\,\mathrm{d}V$ is the linear momentum of a fluid element, and $\times$ is the vector cross product from Cartesian vector analysis. For thermodynamic coordinates $(q^1, q^2, q^3) = (S, \Theta, p)$, with $\mathrm{d}\mathcal{V} = \mathrm{d}S \wedge \mathrm{d}\Theta \wedge \mathrm{d}p$, the water mass angular momentum is

$$L_1 = (\Theta\,\dot{p} - p\,\dot{\Theta})\,\mathfrak{m}\,\mathrm{d}\mathcal{V} \tag{74a}$$

$$L_2 = (p\,\dot{S} - S\,\dot{p})\,\mathfrak{m}\,\mathrm{d}\mathcal{V} \tag{74b}$$

$$L_3 = (S\,\dot{\Theta} - \Theta\,\dot{S})\,\mathfrak{m}\,\mathrm{d}\mathcal{V}. \tag{74c}$$

Likewise, the $N = 2$ configuration space with $(q^1, q^2) = (S, \Theta)$ and $\mathrm{d}\mathcal{V} = \mathrm{d}S \wedge \mathrm{d}\Theta$ has

$$L = (S\,\dot{\Theta} - \Theta\,\dot{S})\,\mathfrak{m}\,\mathrm{d}\mathcal{V}. \tag{75}$$

The $\boldsymbol{q}$-space angular momentum satisfies the following properties.

- For each elemental region of water mass space, the $\boldsymbol{q}$-space angular momentum is built from the mass of the region multiplied by a couplet that measures the local $\boldsymbol{q}$-space rotation. In Figure 8 we illustrate the S/Θ couplet for the $N = 2$ water mass space angular momentum given by equation (75).

- The physical dimensions of the water mass angular momentum depend on the dimensions of the water mass coordinates, with the different L_α components for the $N = 3$ case generally having distinct dimensions.

- For $N = 3$ the angular momentum satisfies

$$q^\alpha L_\alpha = 0, \tag{76}$$

which follows since

$$\epsilon_{\alpha\beta\gamma}\, q^\alpha\, q^\beta\, \dot{q}^\gamma = \boldsymbol{q} \cdot (\boldsymbol{q} \times \dot{\boldsymbol{q}}) = 0. \tag{77}$$

It is straightforward to also show that

$$\dot{q}^\alpha L_\alpha = 0 \quad \text{and} \quad q^\alpha \dot{L}_\alpha = 0. \tag{78}$$

Each property also holds for the angular momentum of a fluid element in $\boldsymbol{x}$-space.

- The $\boldsymbol{x}$-space angular momentum depends on the location in space about which the angular momentum is computed. This dependence reflects the subjectivity of the choice for origin when defining angular momentum. Correspondingly, a constant shift in the definition of a water mass coordinate, such as for Absolute Temperature shifted from Kelvin to Celsius, shifts the value of the water mass angular momentum. In Section 5b, we find that for steady flow, the global integral of the water mass angular momentum remains invariant to the choice of origin.

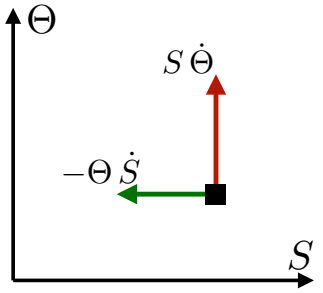

FIG. 8. An example of the S/Θ couplet that forms the angular momentum (equation (75)) for an elemental region of (S, Θ) water mass configuration space. The couplet is represented by a horizontal arrow for the $-\Theta\,\dot{S}$ contribution since $\dot{S}$ measures the rate that fluid moves along the S-axis. Likewise, we depict the contribution from $S\,\dot{\Theta}$ as a vertical arrow. For example, with $S > 0$ and $\Theta > 0$, processes that lead to a material increase in Θ (i.e., $\dot{\Theta} > 0$) with an associated decrease in S (i.e., $\dot{S} < 0$) lead to an increase in angular momentum, $L = (S\,\dot{\Theta} - \Theta\,\dot{S})\,\mathfrak{m}\,\mathrm{d}\mathcal{V}$.

b. $N = 2$ *with steady and source-free flow*

Consider the case of a steady and source-free flow with an $N = 2$ dimensional water mass configuration space. In this case, equation (69) provides a streamfunction so that the angular momentum is given by

$$\begin{aligned}
L &= \epsilon_{\beta\gamma}\, q^\beta\, \dot{q}^\gamma\, \mathfrak{m}\, \mathrm{d}\mathcal{V} && \text{(79a)}\\
&= \epsilon_{\beta\gamma}\, q^\beta\, \epsilon^{\gamma\zeta}\, \partial_\zeta \psi\, \mathrm{d}\mathcal{V} && \text{(79b)}\\
&= -(\epsilon_{1\beta}\, \epsilon^{1\zeta} + \epsilon_{2\beta}\, \epsilon^{2\zeta})\, q^\beta\, \partial_\zeta \psi\, \mathrm{d}\mathcal{V} && \text{(79c)}\\
&= -(q^1\, \partial\psi/\partial q^1 + q^2\, \partial\psi/\partial q^2)\, \mathrm{d}\mathcal{V} && \text{(79d)}\\
&= -\boldsymbol{q} \cdot \nabla_{\boldsymbol{q}} \psi\, \mathrm{d}\mathcal{V} && \text{(79e)}\\
&= -\nabla_{\boldsymbol{q}} \cdot (\boldsymbol{q}\psi)\, \mathrm{d}\mathcal{V} + 2\psi\, \mathrm{d}\mathcal{V}, && \text{(79f)}
\end{aligned}$$

where for the final step we used $\nabla_{\boldsymbol{q}} \cdot \boldsymbol{q} = \partial q^1/\partial q^1 + \partial q^2/\partial q^2 = 2$. Recall from Section 2e that the boundaries of water mass configuration space are assumed to be outside the range where seawater exists. Hence, if we integrate the angular momentum (79f) over all of water mass space, then the total derivative term drops out since the streamfunction vanishes where there is no seawater. We are thus led to

$$\int L = 2 \int \psi\, \mathrm{d}\mathcal{V}, \tag{80}$$

so that in the absence of mass sources, the globally integrated steady state water mass angular momentum equals twice the integrated circulation streamfunction. To within an arbitrary sign for the streamfunction, the result (80) agrees with the angular momentum computed for a non-divergent depth-integrated ocean using $\boldsymbol{x}$-space coordinates (Holloway and Rhines 1991).

Under a constant shift in the water mass coordinates, $\boldsymbol{q} \to \boldsymbol{q} + \boldsymbol{\xi}$ with $\boldsymbol{\xi}$ a constant, the steady state water mass angular momentum (79f) shifts by

$$L \to L - \nabla_{\boldsymbol{q}} \cdot (\boldsymbol{\xi}\psi)\, \mathrm{d}\mathcal{V}, \tag{81}$$

with the extra term vanishing when integrated globally. Hence, the steady state globally integrated water mass angular momentum remains invariant under a constant shift in the origin of the water mass coordinates.

c. $N = 3$ *with steady and source-free flow*

We find an analogous result for the $N = 3$ case after a few more manipulations. In this case we make use of the water mass streamfunction, $\mathfrak{m}\,\dot{q}^\gamma = \epsilon^{\gamma\zeta\eta}\, \partial_\zeta \psi_\eta$ (equation (71)), so that the steady and source-free water mass angular momentum is

$$\begin{aligned}
L_\alpha &= \epsilon_{\alpha\beta\gamma}\, q^\beta\, \dot{q}^\gamma\, \mathfrak{m}\, \mathrm{d}\mathcal{V} && \text{(82a)}\\
&= \epsilon_{\gamma\alpha\beta}\, q^\beta\, \epsilon^{\gamma\zeta\eta}\, \partial_\zeta \psi_\eta\, \mathrm{d}\mathcal{V} && \text{(82b)}\\
&= (\delta^\zeta_\alpha\, \delta^\eta_\beta - \delta^\eta_\alpha\, \delta^\zeta_\beta)\, q^\beta\, \partial_\zeta \psi_\eta\, \mathrm{d}\mathcal{V} && \text{(82c)}\\
&= (q^\eta\, \partial_\alpha \psi_\eta - q^\zeta\, \partial_\zeta \psi_\alpha)\, \mathrm{d}\mathcal{V} && \text{(82d)}\\
&= q^\beta\, (\partial_\alpha \psi_\beta - \partial_\beta \psi_\alpha)\, \mathrm{d}\mathcal{V}, && \text{(82e)}
\end{aligned}$$

where the third equality made use of the identity between the permutation symbol and Kronecker delta

$$\epsilon_{\gamma\alpha\beta}\,\epsilon^{\gamma\zeta\eta} = \delta^{\zeta}_{\alpha}\,\delta^{\eta}_{\beta} - \delta^{\eta}_{\alpha}\,\delta^{\zeta}_{\beta}. \tag{83}$$

Moving the derivatives off the streamfunction yields

$$L_\alpha = [\partial_\alpha(q^\beta\,\psi_\beta) - \partial_\beta(q^\beta\,\psi_\alpha) + 2\psi_\alpha]\,\mathrm{d}\mathcal{V}, \tag{84}$$

where we used equation (5). When integrating globally over $\boldsymbol{q}$-space the derivative terms drop out, thus yielding the angular momentum

$$\int L_\alpha = 2\int \psi_\alpha\,\mathrm{d}\mathcal{V}. \tag{85}$$

We thus find that for a steady and source-free flow, each component of the integrated $\boldsymbol{q}$-space angular momentum is given by twice the integrated streamfunction.

d. $\boldsymbol{q}$-space vs $\boldsymbol{x}$-space angular momentum

As already noted, the $\boldsymbol{q}$-space angular momentum for $N = 3$ is directly analogous to the angular momentum in $\boldsymbol{x}$-space. However, the $\boldsymbol{q}$-space angular momentum is *not* a coordinate transformation of the $\boldsymbol{x}$-space angular momentum. Rather, it is a distinct object that lives in water mass configuration space and is defined whether or not the function $\mathfrak{q}$ from $\mathcal{X}$ to $\mathcal{Q}$ is bijective. Even so, the $\boldsymbol{q}$-space angular momentum shares certain properties with its $\boldsymbol{x}$-space sibling, with further connections seen when studying tracer angular momentum in Section 7f.

6. Tracer equation in q-space

To study tracer budgets in water mass configuration space, we introduce the tracer transport 2-form for $N = 3$

$$\begin{aligned}\mathcal{T}_C &= \mathfrak{m}\,(\dot{q}^1\,C + F^1)\,\mathrm{d}q^2 \wedge \mathrm{d}q^3 \\ &\quad + \mathfrak{m}\,(\dot{q}^2\,C + F^2)\,\mathrm{d}q^3 \wedge \mathrm{d}q^1 \\ &\quad + \mathfrak{m}\,(\dot{q}^3\,C + F^3)\,\mathrm{d}q^1 \wedge \mathrm{d}q^2,\end{aligned} \tag{86}$$

where $\mathfrak{m}\,F^\alpha(\boldsymbol{q}, t)$ are components of a subgrid scale flux for tracer, C. If we set C to a constant and assume the subgrid scale flux vanishes with constant C, then the tracer transport in equation (86) reduces to the mass transport in equation (46). We thus mathematically interpret the tracer transport just as for the mass transport, only now with the added subgrid contribution.

In regions of $\boldsymbol{x}$-space where the mapping to $\boldsymbol{q}$-space is 1-to-1 (with $N = 3$), we can relate the Cartesian subgrid scale flux components to the $\boldsymbol{q}$-space components according to the chain-rule coordinate transformation from tensor analysis

$$F^\alpha(\boldsymbol{q}) = \hat{F}^\alpha(\boldsymbol{x}) = \frac{\partial \mathfrak{q}^\alpha}{\partial x^a}\,F^a(\boldsymbol{x}) = \nabla q^\alpha \cdot \boldsymbol{F}(\boldsymbol{x}), \tag{87}$$

where $\boldsymbol{x} = \mathfrak{x}(\boldsymbol{q}) = \mathfrak{q}^{-1}(\boldsymbol{q})$, $\rho\,F^a$ are the Cartesian components of the subgrid flux, and $\hat{F}^\alpha$ denotes F^α considered as a function of $\boldsymbol{x}$ (which is how it is evaluated in practice).

More generally, when the mapping from $\boldsymbol{x}$-space to $\boldsymbol{q}$-space is not 1-to-1 (such as when $N \neq 3$), the components to the subgrid scale tracer flux in $\boldsymbol{q}$-space are found by following the sifting approach from Section 3d. That is, the generalized subgrid flux in $\boldsymbol{q}$-space is the mass-weighted average of the subgrid flux in $\boldsymbol{x}$-space over regions $\boldsymbol{x} \in \mathcal{X}$ where $\mathfrak{q}(\boldsymbol{x}) = \boldsymbol{q}$,

$$(F^\alpha)^{\text{gen}}(\boldsymbol{q})\;\mathfrak{m}^{\text{gen}}(\boldsymbol{q}) = \int_{\mathcal{X}} \rho(\boldsymbol{x})\,\hat{F}^\alpha(\boldsymbol{x})\,\delta_{\boldsymbol{q}}\big(\mathfrak{q}(\boldsymbol{x})\big)\,\mathrm{d}V. \tag{88}$$

As noted at the end of Section 3d, in the subsequent development we drop the "gen" notation for brevity.

Following the same manipulations as in Section 4b used for the mass continuity equation leads to the tracer continuity equation in $\boldsymbol{q}$-space

$$\partial_t(\mathfrak{m}\,C) = -\partial_\alpha(\mathfrak{m}\,C\,\dot{q}^\alpha + \mathfrak{m}\,F^\alpha) + \mathfrak{m}\,\mathcal{S}_{\text{pure}} + \mathcal{M}\,C_{\text{input}}. \tag{89}$$

We introduced a tracer source, $\mathcal{S}_{\text{pure}}$, with physical dimensions of tracer per time, along with a source, $\mathcal{M}\,C_{\text{input}}$, arising from the tracer contained in the mass source. Radiation is an example tracer source, $\mathcal{S}_{\text{pure}}$, that is independent of the mass source. Making use of the mass continuity equation (55) yields the advective expression of the tracer equation

$$(\partial_t + \dot{q}^\alpha\,\partial_\alpha)\,C = -\mathfrak{m}^{-1}\,\partial_\alpha(\mathfrak{m}\,F^\alpha) + \mathcal{S}, \tag{90}$$

where the combined tracer source is given by

$$\mathfrak{m}\,\mathcal{S} = \mathfrak{m}\,\mathcal{S}_{\text{pure}} + \mathcal{M}\,(C_{\text{input}} - C). \tag{91}$$

Notice that if the tracer concentration associated with the input mass source equals to the ambient tracer concentration, then $\mathfrak{m}\,\mathcal{S} = \mathfrak{m}\,\mathcal{S}_{\text{pure}}$. Also note that setting the tracer concentration to a constant reduces the tracer equation (89) to the corresponding flux form of mass continuity given by equation (55).

The convergence of the subgrid scale flux found in equation (90) is given by

$$\mathcal{D} \equiv -\mathfrak{m}^{-1}\,\partial_\alpha(\mathfrak{m}\,F^\alpha). \tag{92}$$

When the subgrid scale flux is given in the downgradient diffusive form, as in Section 7b ahead, then $\mathcal{D}$ is a generalized Laplacian operator applied to the tracer C. In Appendix A we offer examples of this operator.

7. Water mass configuration space as tracer space

We now study the case where water mass configuration space is defined by N tracer coordinates,

$$\boldsymbol{q} = \boldsymbol{C} = (C^1, \ldots, C^N) \Longleftrightarrow q^\alpha = C^\alpha \quad \alpha = 1, \ldots, N, \tag{93}$$

with the Jacobian and mass density

$$\mathcal{J} = \frac{\partial \boldsymbol{x}}{\partial \boldsymbol{C}} \quad \text{and} \quad \mathfrak{m} = \rho\, |\mathcal{J}| \tag{94}$$

and the mass continuity equation (55)

$$\partial_t \mathfrak{m} = -\partial_\alpha (\mathfrak{m}\, \dot{C}^\alpha) + \mathcal{M}. \tag{95}$$

Recall that if the function $\mathfrak{q}$ from $\mathcal{X}$ to $\mathcal{Q}$ is not bijective, as when $N \neq 3$, then we can patch regions together by following the methods from Section 3d. Thus, we make use of the generalized Jacobian from equation (31) when $N = 3$, or when N is arbitrary we use equation (35) in the discrete case and equation (42) in the continuous case.

a. The tracer equation

With $\boldsymbol{q} = \boldsymbol{C}$, the tracer equation (90) becomes

$$\mathfrak{m}\, (\partial_t + \dot{C}^\alpha\, \partial_\alpha)\, C^\beta = -\partial_\alpha (\mathfrak{m}\, F^{\alpha\beta}) + \mathfrak{m}\, \mathcal{S}^\beta, \tag{96}$$

where $\mathfrak{m}\, F^{\alpha\beta}$ is the α-th component of the subgrid flux for tracer C^β, and $\mathcal{S}^\beta$ is the source for tracer C^β. Since tracers now act as coordinates, the tracer equation (96) simplifies to

$$\mathfrak{m}\, \dot{C}^\beta = -\partial_\alpha (\mathfrak{m}\, F^{\alpha\beta}) + \mathfrak{m}\, \mathcal{S}^\beta, \tag{97}$$

which follows since the partial time derivative, ∂_t, is computed holding each of the tracer coordinates fixed ($\partial_t C^\alpha = 0$), and since $\partial_\alpha\, C^\beta = \delta^\beta_\alpha$ (see equation (5)).

If $\mathfrak{q}$ is bijective, then $F^{\alpha\beta}(\boldsymbol{q})$ is given similarly to $F^\alpha(\boldsymbol{q})$ in (87) but with $\rho \boldsymbol{F}$ replaced by $\rho \boldsymbol{F}^\beta$, the subgrid flux for tracer C^β; otherwise we use the generalized form $(F^{\alpha\beta})^{\text{gen}}(\boldsymbol{q})$ which is similarly modified from the expression for $(F^\alpha)^{\text{gen}}(\boldsymbol{q})$ in equation (88).

b. Subgrid tracer flux

We suppose a flux-gradient relation for the subgrid tracer flux by introducing a kinematic diffusion tensor, $\mathbb{K}$, which is a symmetric and positive definite second order tensor. We also assume the same diffusion tensor is used for all tracers. The latter assumption is valid if all mixing is ultimately achieved by small scale isotropic turbulence (e.g., Davis 1994; Gregg et al. 2018), whereby the turbulent diffusivity is equal for all tracers (see in particular Sections 2.5, 8.5, and Figure 14 from Gregg et al. (2018)). However, if the turbulence is very weak or absent, in which case molecular diffusion is a relatively large contributor to tracer mixing, then different tracers can have different diffusivities. For example, the molecular thermal diffusivity in water is roughly 100 times larger than the salt diffusivity (Gill 1982), which then leads to double-diffusive convection in quiescent ocean regions (Schmitt 1994).

An anti-symmetric component to the mixing tensor is often included in numerical ocean models (Griffies 1998, 2004; Groeskamp et al. 2019). This skew-diffusion is aimed at rendering stirring processes not captured by a model's resolved flow (see Section 2.3 of Groeskamp et al. (2019)). We here focus on mixing parameterized by a symmetric diffusion tensor since it directly leads to transport across tracer surfaces (and thus to water mass transformation), whereas the anti-symmetric skew diffusion tensor is equivalent to an advection.

Representing the subgrid flux for tracer C^β in terms of its $\boldsymbol{x}$-space coordinates yields

$$F^{a\beta} = -\mathbb{K}^{ab}\, \partial_b C^\beta, \tag{98}$$

where $\mathbb{K}^{ab}$ is the $\boldsymbol{x}$-space representation of the diffusion tensor that has dimensions $L^2\, T^{-1}$.

If $\mathfrak{q}$ is bijective, the diffusion tensor can be represented in tracer coordinates through the coordinate transformation

$$\begin{aligned} \mathbb{K}^{\alpha\beta}(\boldsymbol{q}) &= \hat{\mathbb{K}}^{\alpha\beta}\big(\mathfrak{x}(\boldsymbol{q})\big) \\ &= \partial_a C^\alpha\, \mathbb{K}^{ab}\, \partial_b C^\beta = \nabla C^\alpha \cdot \mathbb{K} \cdot \nabla C^\beta. \end{aligned} \tag{99}$$

Similarly to equation (87), we introduce $\hat{\mathbb{K}}^{\alpha\beta}$ to denote $\mathbb{K}^{\alpha\beta}$ considered as a function of $\boldsymbol{x}$; again $\hat{\mathbb{K}}^{\alpha\beta}$ exists whether or not $\mathfrak{q}$ is bijective. The tracer coordinate representation of the subgrid flux then satisfies

$$\mathfrak{m}\, F^{\beta\alpha} = -\mathfrak{m}\, \mathbb{K}^{\alpha\beta} = \mathfrak{m}\, F^{\alpha\beta} \tag{100}$$

by applying equations (98) and (99) to the coordinate transformation equation (87), and using the symmetry of $\mathbb{K}^{ab}$ and hence $\mathbb{K}^{\alpha\beta}$ for the last equality. We thus see that the tracer space representation of the subgrid flux tensor is minus the tracer space representation of the diffusion tensor. Note again that this identity (and the symmetry of $\mathbb{K}^{\alpha\beta}$) requires that the same diffusion tensor applies to each tracer.

If $\mathfrak{q}$ is not bijective, we substitute equation (98) into the expression (88) for $(F^{\alpha\beta})^{\text{gen}}(\boldsymbol{q})$ to give

$$\begin{aligned} &(F^{\alpha\beta})^{\text{gen}}(\boldsymbol{q})\, \mathfrak{m}^{\text{gen}}(\boldsymbol{q}) \\ &\quad = \int_{\mathcal{X}} \rho(\boldsymbol{x})\, \partial_a C^\alpha\, F^{a\beta}\, \delta_{\boldsymbol{q}}\big(\mathfrak{q}(\boldsymbol{x})\big)\, \mathrm{d}V && \text{(101a)} \\ &\quad = -\int_{\mathcal{X}} \rho(\boldsymbol{x})\, \partial_a C^\alpha\, \mathbb{K}^{ab}\, \partial_b C^\beta\, \delta_{\boldsymbol{q}}\big(\mathfrak{q}(\boldsymbol{x})\big)\, \mathrm{d}V && \text{(101b)} \\ &\quad = -\int_{\mathcal{X}} \rho(\boldsymbol{x})\, \hat{\mathbb{K}}^{\alpha\beta}(\boldsymbol{x})\, \delta_{\boldsymbol{q}}\big(\mathfrak{q}(\boldsymbol{x})\big)\, \mathrm{d}V. && \text{(101c)} \end{aligned}$$

We define the generalized diffusion tensor, $(\mathbb{K}^{\alpha\beta})^{\text{gen}}$, as a mass-weighted mean of $\hat{\mathbb{K}}^{\alpha\beta}(\boldsymbol{x})$ over regions $\boldsymbol{x} \in \mathcal{X}$ where $\mathfrak{q}(\boldsymbol{x}) = \boldsymbol{q}$:

$$(\mathbb{K}^{\alpha\beta})^{\text{gen}}(\boldsymbol{q})\, \mathfrak{m}^{\text{gen}}(\boldsymbol{q}) = \int_{\mathcal{X}} \rho(\boldsymbol{x})\, \hat{\mathbb{K}}^{\alpha\beta}(\boldsymbol{x})\, \delta_{\boldsymbol{q}}\big(\mathfrak{q}(\boldsymbol{x})\big)\, \mathrm{d}V. \quad (102)$$

Comparing equations (101c) and (102) shows that $(F^{\alpha\beta})^{\text{gen}}$ and $(\mathbb{K}^{\alpha\beta})^{\text{gen}}$ still obey equation (100) and are symmetric, as long as all tracers are diffused by the same, symmetric, $\mathbb{K}$. Therefore, in the following we again drop the "gen" notation.

The corresponding representation of the diffusion operator, equation (92), acting on tracer C^β is given by

$$-\mathfrak{m}^{-1}\, \partial_\alpha(\mathfrak{m}\, F^{\alpha\beta}) = \mathfrak{m}^{-1}\, \partial_\alpha(\mathfrak{m}\, \mathbb{K}^{\alpha\beta}). \quad (103)$$

Note that these relations were also used by Mackay et al. (2018, 2020) in an oceanographic inverse study.

c. *Variances and covariances for $\boldsymbol{q} = (S, \Theta)$ without sources*

Consider the tracer equation (97) for the $N = 2$ tracer space with $\boldsymbol{q} = (S, \Theta)$, and suppose there are no tracer sources (whether interior or boundary). The two tracer equations are

$$\mathfrak{m}\, \dot{S} = -\partial_S(\mathfrak{m}\, F^{SS}) - \partial_\Theta(\mathfrak{m}\, F^{\Theta S}), \quad (104a)$$

$$\mathfrak{m}\, \dot{\Theta} = -\partial_S(\mathfrak{m}\, F^{S\Theta}) - \partial_\Theta(\mathfrak{m}\, F^{\Theta\Theta}). \quad (104b)$$

For the salinity equation, its two flux components, $\mathfrak{m}\, F^{\alpha S}$, include F^{SS}, arising from the subgrid flux of S in the S direction, and $F^{\Theta S}$, arising from the subgrid flux of S in the Θ direction. The Θ equation has similar flux components.

We expose some properties of the subgrid flux components by studying how they affect the evolution of tracer variance (squared tracer) and tracer covariance (product of two different tracers) (see Ruan and Ferrari (2021) for an analogous discussion). Start by considering the evolution equation for one-half the squared salinity, which is readily derived from the salinity equation (104a),

$$\mathfrak{m}\, S\, \dot{S} = -\partial_\alpha(\mathfrak{m}\, S\, F^{\alpha S}) + \mathfrak{m}\, F^{SS}, \quad (105)$$

where $S\,\dot{S} = \frac{1}{2}\mathrm{D}(S^2)/\mathrm{D}t$ is half the mass-weighted material evolution of the squared salinity, and we used $\partial_\alpha C^\beta = \delta^\beta_\alpha$ from equation (5). The first term on the RHS of (105) is a flux-convergence term that represents the redistribution of variance. Its global integral vanishes as both the mass density and the subgrid flux vanish outside the regions of $\boldsymbol{q}$-space where seawater exists. The second term is given by (101a) and (101b) as

$$\mathfrak{m}\, F^{SS} = \int_{\mathcal{X}} \rho(\boldsymbol{x})\, \nabla S \cdot \boldsymbol{F}^S\, \delta_{\boldsymbol{q}}\big(\mathfrak{q}(\boldsymbol{x})\big)\, \mathrm{d}V \quad (106a)$$

$$= -\int_{\mathcal{X}} \rho(\boldsymbol{x})\, \nabla S \cdot \mathbb{K} \cdot \nabla S\, \delta_{\boldsymbol{q}}\big(\mathfrak{q}(\boldsymbol{x})\big)\, \mathrm{d}V \le 0, \quad (106b)$$

where the inequality follows for downgradient fluxes in which $\mathbb{K}$ is a symmetric and positive definite diffusion tensor. Hence, in the presence of diffusion, the integral of $\mathfrak{m}\, F^{SS}\, \mathrm{d}\mathcal{V}$ over a finite region of $\boldsymbol{q}$-space provides a sign-definite sink to the evolution of the squared salinity, and hence a sink to salinity variance.

Equation (106b) is reminiscent of the formula (7a) in Winters and D'Asaro (1996) for the flux of a scalar θ across an isosurface of θ per unit horizontal area:

$$\phi_d(\theta) = -\kappa\, \frac{\mathrm{d}z^*}{\mathrm{d}\theta}\, \langle (\nabla\theta)^2 \rangle_\theta, \quad (107)$$

where z^* is the mean height of the θ surface, and in our notation $\phi_d = F^{\theta\theta}$, κ is the (isotropic) diffusivity (i.e. $\mathbb{K}^{ab} = \kappa \delta^{ab}$), and $\langle (\nabla\theta)^2 \rangle_\theta$ represents the thickness-weighted average of $(\nabla\theta)^2$ on the θ surface. In our formalism, $\mathrm{d}z^*/\mathrm{d}\theta$, the volume per unit area per unit θ, represents the generalized Jacobian $\mathrm{d}V/\mathrm{d}\mathcal{V}$ for the transformation from the $N = 3$ configuration space x, y, θ back to $\boldsymbol{x}$-space. Both equations (106b) and (107) emphasize how the flux across a scalar surface is increased by folding and break-up of the surface.

Following similar methods, we readily obtain an evolution equation for the product of $S\Theta$ from equations (104a) and (104b), whereby

$$\mathfrak{m}\, \Theta\, \dot{S} = -\partial_\alpha(\mathfrak{m}\, \Theta\, F^{\alpha S}) + \mathfrak{m}\, F^{\Theta S} \quad (108a)$$

$$\mathfrak{m}\, S\, \dot{\Theta} = -\partial_\alpha(\mathfrak{m}\, S\, F^{\alpha\Theta}) + \mathfrak{m}\, F^{S\Theta}. \quad (108b)$$

The sum $\Theta\,\dot{S} + S\,\dot{\Theta}$ measures changes to the (S, Θ)-covariance when integrated over the ocean domain. Since S and Θ are assumed to be diffused by the same symmetric tensor, with

$$\boldsymbol{F}^S \cdot \nabla\Theta = -\nabla\Theta \cdot \mathbb{K} \cdot \nabla S = \boldsymbol{F}^\Theta \cdot \nabla S, \quad (109)$$

it follows that the S component of the subgrid-scale flux of Θ is equal to the Θ component of the subgrid-scale flux of S:

$$\mathfrak{m}\, F^{S\Theta} = \int_{\mathcal{X}} \rho(\boldsymbol{x})\, \nabla S \cdot \boldsymbol{F}^\Theta\, \delta_{\boldsymbol{q}}\big(\mathfrak{q}(\boldsymbol{x})\big)\, \mathrm{d}V \quad (110a)$$

$$= \int_{\mathcal{X}} \rho(\boldsymbol{x})\, \nabla\Theta \cdot \boldsymbol{F}^S\, \delta_{\boldsymbol{q}}\big(\mathfrak{q}(\boldsymbol{x})\big)\, \mathrm{d}V \quad (110b)$$

$$= \mathfrak{m}\, F^{\Theta S}. \quad (110c)$$

Hence, a salinity flux crossing temperature surfaces causes an evolution of (S,Θ)-covariance, as does a temperature flux crossing salinity surfaces. Since these two fluxes, $\boldsymbol{F}^{\Theta S}$ and $\boldsymbol{F}^{S\Theta}$, are not sign-definite, the globally integrated $S\Theta$ (and hence the (S,Θ)-covariance) can increase or decrease in time, in contrast to the globally integrated squared tracer (and hence tracer variance) which decreases in time.

To summarise, if we measure variance loss in a tracer mixing experiment, diffusive fluxes of salinity are directed down the salinity gradient and diffusive fluxes of temperature are directed down the temperature gradient. In contrast, measured variance gain corresponds to fluxes up the gradient. Measured covariance sources and sinks (sign unclear) reflect diffusive fluxes of salinity that project onto the temperature gradient and fluxes of temperature that project onto the salinity gradient.

d. Mass continuity

Making use of the tracer equation in the form (97) allows us to write the mass continuity equation (95) as

$$\partial_t \mathfrak{m} = -\partial_\alpha \left[\partial_\beta(\mathfrak{m}\,\mathbb{K}^{\alpha\beta}) + \mathfrak{m}\,\mathcal{S}^\alpha\right] + \mathcal{M}. \tag{111}$$

This equation locally connects the evolution of mass within tracer space to the mixing of tracers that acts to move mass across the tracer contours, plus any contributions from tracer and mass sources.

e. Tracer coordinate streamfunction

Now consider a steady tracer space circulation with zero mass source ($\mathcal{M}=0$), in which case the mass continuity (111) reduces to the non-divergence condition

$$0 = -\partial_\alpha[\partial_\beta(\mathfrak{m}\,\mathbb{K}^{\alpha\beta}) + \mathfrak{m}\,\mathcal{S}^\alpha] = \partial_\alpha(\mathfrak{m}\,\dot{C}^\alpha), \tag{112}$$

having used equations (97) and (100) for the second equality. Connecting to the $N=3$ streamfunction in equation (71) leads to

$$\mathfrak{m}\,\dot{C}^\alpha = \epsilon^{\alpha\beta\gamma}\,\partial_\beta\psi_\gamma = \partial_\beta(\mathfrak{m}\,\mathbb{K}^{\alpha\beta}) + \mathfrak{m}\,\mathcal{S}^\alpha, \tag{113}$$

which can be written more succinctly using vector notation

$$\mathfrak{m}\,\dot{\boldsymbol{C}} = \nabla_{\boldsymbol{C}} \times \boldsymbol{\psi} = \nabla_{\boldsymbol{C}} \cdot (\mathfrak{m}\,\hat{\mathbb{K}}) + \mathfrak{m}\,\mathcal{S}. \tag{114}$$

The hat on the diffusion tensor signals that it is represented using tracer coordinates as per equation (99). Equations (113) and (114) reveal that the streamfunction for steady circulation in tracer space is locally related to the diffusion tensor and to the $\boldsymbol{q}$-space tracer sources. This connection follows since tracer mixing, as parameterized by a symmetric diffusion tensor, generates local circulation in tracer space. Also, recall that $\boldsymbol{q}$-space tracer sources reflect the usual $\boldsymbol{x}$-space sources (e.g., biogeochemical sources) as well as $\boldsymbol{x}$-space boundary fluxes. In the absence of any $\boldsymbol{q}$-space tracer sources (including zero $\boldsymbol{x}$-space boundary fluxes), then diffusion leads to a steady state with homogenized tracers and thus to a trivial (zero) $\boldsymbol{q}$-space circulation where $\dot{\boldsymbol{C}} = 0$.

f. Tracer angular momentum

When using tracer coordinates, we refer to the $\boldsymbol{q}$-space angular momentum as the tracer angular momentum, which takes the form

$$L_\alpha = \epsilon_{\alpha\beta\gamma}\, C^\beta\, \dot{C}^\gamma\, \mathfrak{m}\, \mathrm{d}\mathcal{V} \tag{115a}$$

$$= \epsilon_{\alpha\beta\gamma}\, C^\beta \left[-\partial_\zeta(\mathfrak{m}\, F^{\zeta\gamma}) + \mathfrak{m}\,\mathcal{S}^\gamma\right] \mathrm{d}\mathcal{V} \tag{115b}$$

$$= \epsilon_{\alpha\beta\gamma} \left[-\partial_\zeta(\mathfrak{m}\, F^{\zeta\gamma}\, C^\beta) + \mathfrak{m}\,\mathcal{S}^\gamma\, C^\beta\right] \mathrm{d}\mathcal{V}. \tag{115c}$$

For the final step we made use of the identity

$$\epsilon_{\alpha\beta\gamma}\,\partial_\zeta C^\beta\, F^{\zeta\gamma} = \epsilon_{\alpha\beta\gamma}\,\delta^\beta_\zeta\, F^{\zeta\gamma} = \epsilon_{\alpha\beta\gamma}\, F^{\beta\gamma} = 0, \tag{116}$$

which follows from anti-symmetry of $\epsilon_{\alpha\beta\gamma}$ along with symmetry of $F^{\beta\gamma}$ (see equation (100)). The identity (116) is a critical step that allows us to write each component of the tracer angular momentum in equation (115c) as a tracer space convergence plus a source. Hence, integrating over all of tracer space removes contributions from interior diffusive mixing processes, leaving just tracer sources

$$\int L_\alpha = \epsilon_{\alpha\beta\gamma} \int \mathcal{S}^\gamma\, C^\beta\, \mathfrak{m}\, \mathrm{d}\mathcal{V}. \tag{117}$$

Recall that tracer sources in $\boldsymbol{q}$-space correspond to both the $\boldsymbol{x}$-space sources plus $\boldsymbol{x}$-space boundary fluxes. It follows that the global integral for each of the three components to the tracer angular momentum is identically zero when the $\boldsymbol{q}$-space source for the complementary tracers vanish

$$\int L_\alpha = 0 \quad \text{if } \mathcal{S}^\gamma = 0 \text{ for all } \gamma \neq \alpha. \tag{118}$$

g. Tracer angular momentum in $\boldsymbol{x}$-space

We can realize the above result for the tracer angular momentum by integrating over $\boldsymbol{x}$-space rather than tracer space, where Cartesian coordinates leads to

$$L_\alpha = \epsilon_{\alpha\beta\gamma}\, C^\beta \left[-\nabla\cdot(\rho\, \boldsymbol{F}^\gamma) + \rho\,\mathcal{S}^\gamma\right] \mathrm{d}V \tag{119a}$$

$$= \epsilon_{\alpha\beta\gamma} \left[-\nabla\cdot(C^\beta\,\rho\, \boldsymbol{F}^\gamma) + \rho\, C^\beta\,\mathcal{S}^\gamma\right] \mathrm{d}V, \tag{119b}$$

where we used the identity

$$\epsilon_{\alpha\beta\gamma}\,\nabla C^\beta \cdot \boldsymbol{F}^\gamma = -\epsilon_{\alpha\beta\gamma}\,\nabla C^\beta \cdot \mathbb{K} \cdot \nabla C^\gamma = 0. \tag{120}$$

We again see that the global integral of the tracer angular momentum reduces to contributions from $\boldsymbol{x}$-space sources plus $\boldsymbol{x}$-space boundary fluxes.

h. Why diffusion plays no role in global integrated tracer angular momentum

It is remarkable that diffusive mixing cannot engender any globally integrated tracer angular momentum. This null result holds so long as the diffusion tensor is symmetric and the same diffusion tensor is used for each pair of tracers building the angular momentum. Diffusion tensor symmetry ensures that the contribution from diffusion to angular momentum couplets (Figure 8) precisely balance when integrated over the domain. Mathematically, this balance manifests since the local contribution from the diffusive flux appears inside of a total derivative operator.

There is precedent for this result from studying the $\boldsymbol{x}$-space angular momentum. For a Newtonian fluid, the stress tensor is symmetric, which means that stresses do not alter the angular momentum within the fluid interior (see, for example, Section 17.3.3 of Griffies (2004) or Section 2.3.1 of Olbers et al. (2012)). Likewise, we here find that a single symmetric diffusion tensor used for all tracers cannot alter the globally integrated tracer angular momentum. If, furthermore, there are no $\boldsymbol{x}$-space boundary contributions or $\boldsymbol{x}$-space sources, then the integrated tracer angular momentum is zero. Conversely, if we diagnose that the integrated tracer angular momentum is nonzero, then we conclude that either (i) boundary effects or (ii) sources are at play, or that (iii) different tracers have different diffusion tensors. In particular, if two of the tracers are Θ and S and if there are no boundary contributions or sources, then a nonzero integrated tracer angular momentum is a signature of double diffusive processes, in which the diffusivities (either molecular or turbulent) of Θ and S are distinct.

i. Tracer angular momentum in an exchange model

Consider a discrete exchange model for mixing that complements our previous examination of continuous diffusion. In Figure 9 we depict an isolated region with fixed mass M_1 and uniform (S_1, Θ_1), surrounded by fluid with fixed mass M_0 and uniform (S_0, Θ_0). A mass transport, $Q > 0$ (dimensions mass per time), carries fluid through the region, and mass does not converge anywhere. We model the exchange of fluid properties between the small region and large region via upwind exchange, as commonly used for transport in box models such as Stommel (1961).

The above assumptions lead to the (S, Θ) evolution equations

$$M_0 \dot{S}_0 = -Q\,(S_0 - S_1), \quad M_0 \dot{\Theta}_0 = -Q\,(\Theta_0 - \Theta_1) \tag{121a}$$

$$M_1 \dot{S}_1 = Q\,(S_0 - S_1), \quad M_1 \dot{\Theta}_1 = Q\,(\Theta_0 - \Theta_1), \tag{121b}$$

which manifest the conservation of salt and enthalpy for the fixed mass system. The corresponding thermohaline angular momentum component, $L = (S\dot{\Theta} - \Theta\dot{S})\,\mathfrak{m}\,d\mathcal{V}$, for each region is given by

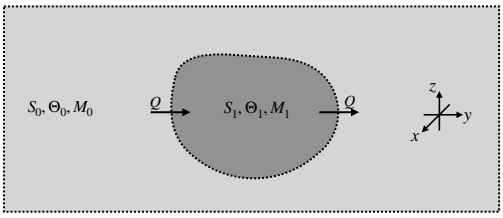

FIG. 9. An isolated region of seawater exposed to mass and tracer transport with the surrounding fluid. Here we consider the case of $\boldsymbol{q} = (S, \Theta, C)$ and focus on the tracer angular momentum component $L = (S\dot{\Theta} - \Theta\dot{S})\,\mathfrak{m}\,d\mathcal{V}$, with C an arbitrary passive tracer. The dark region has uniform (S_1, Θ_1) and fixed mass, M_1, whereas the surrounding fluid has uniform (S_0, Θ_0) and fixed mass, M_0. Fluid moves relative to the dark region with a mass transport, $Q > 0$. Mass does not converge anywhere in the fluid, including the dark region.

$$L_0 = [S_0 \dot{\Theta}_0 - \dot{S}_0 \Theta_0]\, M_0 \tag{122a}$$

$$L_1 = [S_1 \dot{\Theta}_1 - \dot{S}_1 \Theta_1]\, M_1. \tag{122b}$$

Using the upwind time tendencies (121a)–(121b) renders a vanishing net thermohaline angular momentum,

$$L_0 + L_1 = 0. \tag{123}$$

We thus find a precise cancellation of the thermohaline angular momentum generated by the upwind transport through the two regions. This example offers yet another manifestation of how mixing, whether diffusive mixing or exchange mixing, leads to a zero net tracer angular momentum so long as the mixing acts the same for each tracer.

j. Connection to probability angular momentum

Weiss et al. (2019) made use of a probability angular momentum to characterize non-equilibrium steady states found on the configuration space defined by climate indices. In formulating their angular momentum, they made use of a Fokker-Planck equation for the probability density function, and considered both drift and diffusion in this equation. Our approach focuses on the tracer equation rather than the Fokker-Planck equation, though the two are related (e.g., see Section 2.5.2 of van Sebille et al. (2018)). Furthermore, we considered both time-dependent and steady flows. Developing insights into the connection between the two angular momenta is worthy of further research.

8. Summary and conclusions

In this paper we developed a mathematical formalism for water mass configuration space ($\boldsymbol{q}$-space) as defined by an arbitrary number of continuous properties. Since $\boldsymbol{q}$-space generally has no metric, we made use of some rudimentary

features of exterior forms (see Appendix B) in the derivation of $\boldsymbol{q}$-space mass continuity, tracer continuity, steady state streamfunction, and angular momentum. By pursuing the formulation within water mass configuration space, we were able to develop general properties of circulation in $\boldsymbol{q}$-space. Although the mapping from $\boldsymbol{x}$-space to $\boldsymbol{q}$-space is not generally a 1-to-1 coordinate transformation, we detailed a method that renders the same budget equations regardless of the relation between the two spaces. This approach allowed us to expose the underlying mathematical structure of the budget equations and to seamlessly make connections to special cases when the mapping from $\boldsymbol{x}$-space to $\boldsymbol{q}$-space is 1-to-1.

We offered a case study of water mass configuration space defined by tracers. Working in this space reveals a local connection between tracer mixing and circulation in tracer space. That connection is highly constrained when the mixing is parameterized by a single symmetric diffusion tensor, in which case we find that the global integral of the tracer angular momentum is unaffected by diffusive mixing, with this property holding for both steady and time evolving flows. We thus find that although diffusive mixing (along with boundary transport and sources) plays a key role in local water mass transformation (i.e., fluid motion across tracer surfaces), and the local behaviour of tracer angular momentum, only boundary transport and interior sources can alter the globally integrated tracer angular momentum. Consequently, any net tracer angular momentum signals the role of tracer sources or boundary processes, or that mixing of different tracers occurs via different diffusion tensors (e.g., double diffusive processes).

We have revealed fundamental constraints on ocean circulation in a water mass configuration space and hope to have laid mathematical foundations for further advances. We propose that these constraints will be of practical use in observational and numerical model-based descriptions of the ocean's mean circulation (e.g. Groeskamp et al. 2017), its variability (e.g. Evans et al. 2014, 2018) and its response to global warming (e.g. Zika et al. 2021; Sohail et al. 2022) and potentially to other sub-fields of fluid mechanics (e.g. Laliberté et al. 2015). We are motivated to pursue such lines of research and hope this study motivates others as well.

Acknowledgments. We thank the following colleagues for suggestions made at various points of this research: Rebecca Beadling, Henri Drake, Baylor Fox-Kemper, Graeme MacGilchrist, Trevor McDougall, Alberto Naveira Garabato, Charles Nurser, Chris Wilson, and Houssam Yassin. AJGN acknowledges funding from the NERC project (NE/P019293/1) Transient tracer-based Investigation of Circulation and Thermal Ocean Change (TICTOC).

Data availability statement. For Figure 1, we made use of the ACCESS-CM2 climate model of Bi et al. (2020), specifically years 490-499 of the pre-industrial simulation. The circulation makes use of the 3D non-divergent velocity as well as sub-grid scale transport and the local tendency as recommended by Groeskamp et al. (2014). These ACCESS-CM2 data will be made freely available via figshare.com at time of publication. For Figures 3 and 4 we made use of the EN4 analysis product of Good et al. (2013). EN.4.2.2 data were obtained from `https://www.metoffice.gov.uk/hadobs/en4/` and are ©British Crown Copyright, Met Office, provided under a Non-Commercial Government Licence.

APPENDIX A

Example tracer subgrid operators

Our derivation of the subgrid scale tracer operator (92), which made use of exterior calculus, is distinct from those that commonly appear in traditional tensor analysis literature, such as Section 7.56 of Aris (1962) or section 21.5 of Griffies (2004), since here we do not make use of a metric structure nor the corresponding covariant divergence operator. We here exhibit the subgrid operator using the sample $\boldsymbol{q}$-coordinates taken from Section 4c in which we assume the mapping $\mathfrak{q}$ from $\mathcal{X}$ to $\mathcal{Q}$ is bijective. We make use of the transformation (88) between the subgrid scale flux components written in $\boldsymbol{x}$-space and $\boldsymbol{q}$-space. For Cartesian coordinates with $\boldsymbol{q} = \boldsymbol{x}$ and $\mathfrak{m} = \rho$ we have

$$\rho\, \mathcal{D} = -\nabla \cdot (\rho\, \boldsymbol{F}), \tag{A1}$$

with $\nabla = (\partial_x, \partial_y, \partial_z)$. For spherical coordinates, $q^\alpha = (\lambda, \phi, r)$, in which case $\mathfrak{m} = \rho\, r^2 \cos\phi$ and

$$F^\lambda = \nabla\lambda \cdot \boldsymbol{F} = (r\cos\phi)^{-1}\, \hat{\boldsymbol{\lambda}} \cdot \boldsymbol{F} \tag{A2a}$$

$$F^\phi = \nabla\phi \cdot \boldsymbol{F} = r^{-1}\, \hat{\boldsymbol{\phi}} \cdot \boldsymbol{F} \tag{A2b}$$

$$F^r = \nabla r \cdot \boldsymbol{F} = \hat{\boldsymbol{r}} \cdot \boldsymbol{F}, \tag{A2c}$$

with the spherical unit vectors written in terms of the Cartesian unit vectors

$$\hat{\boldsymbol{\lambda}} = -\hat{\boldsymbol{x}} \sin\lambda + \hat{\boldsymbol{y}} \cos\lambda \tag{A3a}$$

$$\hat{\boldsymbol{\phi}} = -\hat{\boldsymbol{x}} \cos\lambda \sin\phi - \hat{\boldsymbol{y}} \sin\lambda \sin\phi + \hat{\boldsymbol{z}} \cos\phi \tag{A3b}$$

$$\hat{\boldsymbol{r}} = \hat{\boldsymbol{x}} \cos\lambda \cos\phi + \hat{\boldsymbol{y}} \sin\lambda \cos\phi + \hat{\boldsymbol{z}} \sin\phi. \tag{A3c}$$

The subgrid operator is thus given by

$$\begin{aligned}(\rho\, r^2 \cos\phi)\, \mathcal{D} = &-r\, \partial_\lambda\, (\rho\, \hat{\boldsymbol{\lambda}} \cdot \boldsymbol{F}) \\ &- r\, \partial_\phi\, (\rho \cos\phi\, \hat{\boldsymbol{\phi}} \cdot \boldsymbol{F}) - \cos\phi\, \partial_r\, (r^2\, \hat{\boldsymbol{r}} \cdot \boldsymbol{F}),\end{aligned} \tag{A4}$$

Finally, for generalized vertical coordinates, $q^\alpha = (x, y, \sigma)$, in which case $\mathfrak{m} = \rho\, (\partial z/\partial\sigma)$ so that

$$\rho\, (\partial z/\partial\sigma)\, \mathcal{D} = -\partial_\alpha [\rho\, (\partial z/\partial\sigma)\, F^\alpha], \tag{A5}$$

with the generalized vertical coordinate representation of the flux given in terms of the Cartesian representation

$$F^x = \hat{\boldsymbol{x}} \cdot \boldsymbol{F} \qquad F^y = \hat{\boldsymbol{y}} \cdot \boldsymbol{F} \qquad F^\sigma = \nabla\sigma \cdot \boldsymbol{F}. \tag{A6}$$

APPENDIX B

Exterior forms, exterior algebra, and exterior calculus

In this appendix we provide a tutorial on *exterior forms*, which are also known as *differential forms*. Exterior forms are anti-symmetrized tensors that offer a rich, and physically useful, mathematical structure. They are central to the exterior algebra (also known as the Grassmann algebra) and the corresponding exterior calculus. We are concerned just with exterior forms in space, which conforms to a conventional study of classical mechanics where time is universal and thus has the same value regardless the chosen spatial coordinates, even if the spatial coordinates are time dependent. For simplicity, we use Cartesian coordinates. However, all results in this appendix hold regardless the coordinate choice, which is one of the key powers of exterior forms.

There is a rich literature in physics making use of exterior forms, with Flanders (1989) an early reference that features applications to thermodynamics, fluid mechanics, and Hamiltonian dynamics. Other treatments can be found in the general relativity text by Misner et al. (1973), the mathematical physics texts by Schutz (1980) and Frankel (2012), and the mathematics text by Fortney (2018). Warnick et al. (1997) and Warnick and Russer (2014) provide pedagogical treatments of electrodynamics using exterior forms, with their treatment of great use for our purposes. We also note that Cotter and Thuburn (2014) make use of exterior forms to derive novel numerical methods for the rotating shallow water equations.

Our discussion is terse and relatively superficial since we only require a small portion of the technology for this paper. Even so, we hope this appendix offers a useful entrée to the subject for the mathematically curious reader.

B1. Introducing exterior forms

An exterior p-form is a covariant p-tensor that is anti-symmetric on all of its arguments. Sometimes we drop the "exterior" for brevity, thus referring just to p-forms. Although this definition may mean little to many readers, it turns out that exterior forms are actually quite familiar since they naturally appear inside of integrals. For example, a path integral along a curve, $\int_C (A\,\mathrm{d}x + B\,\mathrm{d}y + C\,\mathrm{d}z)$, in three dimensional space has an integrand defining an exterior 1-form

$$\mathfrak{A} \equiv A\,\mathrm{d}x + B\,\mathrm{d}y + C\,\mathrm{d}z, \tag{B1}$$

where the smooth functions A, B, C are called the coefficients of $\mathfrak{A}$ and $\mathrm{d}x, \mathrm{d}y, \mathrm{d}z$ are differential increments of a Cartesian coordinate basis for three-dimensional Euclidean space. We say that equation (B1) provides a Cartesian coordinate expression for the exterior 1-form $\mathfrak{A}$. Likewise, a surface integral, $\int_S [P\,\mathrm{d}y\,\mathrm{d}z + Q\,\mathrm{d}z\,\mathrm{d}x + R\,\mathrm{d}x\,\mathrm{d}y]$, leads to an exterior 2-form

$$\mathfrak{B} \equiv P\,\mathrm{d}y \wedge \mathrm{d}z + Q\,\mathrm{d}z \wedge \mathrm{d}x + R\,\mathrm{d}x \wedge \mathrm{d}y, \tag{B2}$$

where $\wedge$ is the exterior (or wedge) product described below, with the exterior product carrying the anti-symmetry property of the 2-form. The volume integral, $\int_{\mathcal{V}} H\,\mathrm{d}x\,\mathrm{d}y\,\mathrm{d}z$, leads to an exterior 3-form

$$\mathfrak{C} \equiv H\,\mathrm{d}x \wedge \mathrm{d}y \wedge \mathrm{d}z. \tag{B3}$$

Spaces with higher dimensions, $N > 3$, allow for higher order exterior forms. Note that the wedge product is associative, so that (B3) is unambiguous.

B2. The exterior product and orientation

Building anti-symmetry into the definition of p-forms renders information about orientation of geometric objects such as surfaces and volumes. Orientation is introduced into p-forms (with $p > 1$) through use of the exterior product, which is also known as the wedge product or Grassmann product. The exterior product of two 1-forms, φ and ζ, produces a 2-form by defining the exterior product as the anti-symmetrized tensor (or outer) product

$$\varphi \wedge \zeta = \varphi \otimes \zeta - \zeta \otimes \varphi, \tag{B4}$$

so that

$$\varphi \wedge \zeta = -\zeta \wedge \varphi \Longrightarrow \varphi \wedge \varphi = 0. \tag{B5}$$

Note that we used anti-symmetry of the exterior product to put differentials of the 2-form (B2) into right-handed cyclic order.

When placed inside of an integral, the area and volume element forms are defined by their familiar expressions from multi-variate calculus, yet with a sign (the orientation) carried by the exterior product according to a chosen "standard ordering". We choose $1, 2, 3$ (i.e. x, y, z) to be the standard ordering. Hence, the oriented volume integral of an arbitrary function, Φ, is written

$$\int \Phi\,\mathrm{d}x \wedge \mathrm{d}y \wedge \mathrm{d}z = \int \Phi\,\mathrm{d}x\,\mathrm{d}y\,\mathrm{d}z = \int \Phi\,\mathrm{d}V, \tag{B6}$$

whereas an odd permutation incurs a minus sign so that

$$-\int \Phi\,\mathrm{d}y \wedge \mathrm{d}x \wedge \mathrm{d}z = \int \Phi\,\mathrm{d}x \wedge \mathrm{d}y \wedge \mathrm{d}z = \int \Phi\,\mathrm{d}V. \tag{B7}$$

In ordinary vector analysis we make use of a surface normal vector, such as $\hat{\boldsymbol{z}}$, to orient a surface in either the

positive or negative $\hat{\boldsymbol{z}}$ directions. Anti-symmetry of the exterior product provides the exterior 2-form, $\mathrm{d}x \wedge \mathrm{d}y$, with the ability to both measure the area of the surface element and to orient the surface in space so that a normal vector is unnecessary. Thinking about the right hand rule, the exterior product incorporates the wrapping of the first and second fingers, and in so doing captures the orientation sense (clockwise or counter-clockwise). However, the exterior product jettisons the thumb since orientation only requires information within the surface and does not require information about directions outside the surface. We can thus conceive of the exterior product as enabling a thumb-less right hand rule.

The 3-form, $\mathrm{d}x \wedge \mathrm{d}y \wedge \mathrm{d}z$, is the oriented volume element for Euclidean three-space. A 3-form is the highest order exterior form available in three-dimensional space. The reason is that p-forms with $p > N$ all vanish due to anti-symmetry. It follows that all p-forms with $p = N$ are directly proportional to the volume form.

B3. The interior product

A (covariant) 1-form $\alpha = \alpha_i \mathrm{d}x^a$ is *dual* to a (contravariant) vector $\boldsymbol{v} = v^a \partial/\partial x^a$, with the contraction

$$\alpha(\boldsymbol{v}) = \alpha_a v^a = s, \tag{B8}$$

where s is a scalar (0-form). This contraction can be generalised to the interior product, $i_{\mathbf{v}}\alpha$, which takes a p-form α to a $(p-1)$-form by contracting the vector, $\boldsymbol{v}$, with the first index of α. If the p-form is the exterior product of a q-form β and a $(p-q)$-form γ the interior product is given by

$$i_{\mathbf{v}}(\beta \wedge \gamma) = [i_{\mathbf{v}}\beta] \wedge \gamma + (-1)^q \beta \wedge [i_{\mathbf{v}}\gamma]\,. \tag{B9}$$

Where the p-form is built up as sequence of 1-forms, its interior product can be expanded by (possibly repeated) application of (B9). For instance

$$\begin{aligned} i_{\mathbf{v}}(A\mathrm{d}x \wedge \mathrm{d}y \wedge \mathrm{d}z) &= [i_{\mathbf{v}}A\mathrm{d}x]\,\mathrm{d}y \wedge \mathrm{d}z - A\mathrm{d}x \wedge [i_{\mathbf{v}}(\mathrm{d}y \wedge \mathrm{d}z)] \\ &= A\,(v^x \mathrm{d}y \wedge \mathrm{d}z + v^y \mathrm{d}z \wedge \mathrm{d}x + v^z \mathrm{d}x \wedge \mathrm{d}y). \end{aligned} \tag{B10}$$

B4. The exterior derivative

The algebra of exterior forms is known as *exterior algebra*, whose properties largely follow from anti-symmetry of the exterior product. Likewise, the calculus of exterior forms is known as *exterior calculus*, whose properties are tied to the *exterior derivative* operator.

a. Exterior derivatives

The differential increment operator, d, is a fundamental part of Riemann integrals since it provides the infinitesimal increment needed to perform the integral. In the study of exterior forms, d is the exterior derivative, which is an anti-symmetrized differential operator that acts on a p-form and produces a $(p+1)$-form. Although the exterior derivative can be extended to both space and time coordinates, we are only concerned with the exterior derivative acting on the spatial coordinates, in which case

$$\mathrm{d} = \left[\mathrm{d}x\,\partial_x + \mathrm{d}y\,\partial_y + \mathrm{d}z\,\partial_z\right] \wedge . \tag{B11}$$

When d is applied to a 0-form (a function), the exterior product reduces to standard scalar multiplication, so the exterior derivative takes the simpler form $\mathrm{d} = \mathrm{d}x^a \partial_a$. To apply d to a p-form (for $p \geq 1$), the coefficients of the p-form combine with the partial derivatives, whereas the differentials of the p-form combine (via the exterior product) with the differentials $\mathrm{d}x$, $\mathrm{d}y$, and $\mathrm{d}z$. Considering equation (B11), the exterior derivative d is like a 1-form, but with partial derivatives for its coefficients.

The squared exterior derivative operator vanishes

$$\mathrm{d}\,\mathrm{d} = \mathrm{d}^2 = 0, \tag{B12}$$

which is a key property we make use of in the following, and we illustrate it in Section B4g.

b. Anti-symmetry of the exterior derivative

Consider the exterior product of an arbitrary p-form, φ, and r-form, ζ. The exterior derivative of this exterior product is

$$\mathrm{d}(\varphi \wedge \zeta) = \mathrm{d}\varphi \wedge \zeta + (-1)^p \varphi \wedge \mathrm{d}\zeta, \tag{B13}$$

thus reflecting the anti-symmetry properties of the exterior derivative when acting across the exterior product. Notably, the exterior derivative picks up the $(-1)^p$ factor as it crosses the p-form, φ, to then act on ζ.

c. Exterior derivative of a 0-form

The exterior derivative of a 0-form (a function) produces a 1-form

$$\mathrm{d}A = (\mathrm{d}x^a\,\partial_a)\,A = \mathrm{d}x\,\partial_x A + \mathrm{d}y\,\partial_y A + \mathrm{d}z\,\partial_z A. \tag{B14}$$

d. Exterior derivative of a 1-form

The exterior derivative of a 1-form yields a 2-form. For example with $\mathfrak{A}$ from equation (B1) we have

$$\mathrm{d}\mathfrak{A} = \mathrm{d}(A\,\mathrm{d}x) + \mathrm{d}(B\,\mathrm{d}y) + \mathrm{d}(C\,\mathrm{d}z) \tag{B15a}$$

$$= \mathrm{d}A \wedge \mathrm{d}x + \mathrm{d}B \wedge \mathrm{d}y + \mathrm{d}C \wedge \mathrm{d}z \tag{B15b}$$

where we dropped the d^2 terms due to the property (B12). The final expression can be expanded by performing the

exterior derivative on the functions A, B, C, thus yielding

$$\begin{aligned} \mathrm{d}\mathfrak{A} &= (\partial_y C - \partial_z B)\,\mathrm{d}y \wedge \mathrm{d}z \\ &\quad + (\partial_z A - \partial_x C)\,\mathrm{d}z \wedge \mathrm{d}x \\ &\quad + (\partial_x B - \partial_y A)\,\mathrm{d}x \wedge \mathrm{d}y. \end{aligned} \tag{B16}$$

This result reveals the connection to the vector curl operation from 3D Cartesian vector analysis.

e. Exterior derivative of a 2-form

The exterior derivative of a 2-form is given by a 3-form. For example, with $\mathfrak{B}$ from equation (B2) we have

$$\mathrm{d}\mathfrak{B} = \mathrm{d}(P\,\mathrm{d}y \wedge \mathrm{d}z) + \mathrm{d}(Q\,\mathrm{d}z \wedge \mathrm{d}x) + \mathrm{d}(R\,\mathrm{d}x \wedge \mathrm{d}y) \tag{B17a}$$

$$= (\partial_x P + \partial_y Q + \partial_z R)\,\mathrm{d}x \wedge \mathrm{d}y \wedge \mathrm{d}z, \tag{B17b}$$

which reveals the connection to the vector divergence operator from 3D Cartesian vector analysis.

f. Exterior derivative of a 3-form

The exterior derivative of a 3-form vanishes in three-dimensional space, which we see by

$$\mathrm{d}\mathfrak{C} = \mathrm{d}(H\,\mathrm{d}V) \tag{B18a}$$

$$= (\partial_x H\,\mathrm{d}x + \partial_y H\,\mathrm{d}y + \partial_z H\,\mathrm{d}z) \wedge \mathrm{d}V \tag{B18b}$$

$$= 0, \tag{B18c}$$

where we wrote the volume 3-form as

$$\mathrm{d}V = \mathrm{d}x \wedge \mathrm{d}y \wedge \mathrm{d}z, \tag{B19}$$

made use of the associativity property of the exterior product, and used anti-symmetry so that

$$\mathrm{d}x \wedge \mathrm{d}x = \mathrm{d}y \wedge \mathrm{d}y = \mathrm{d}z \wedge \mathrm{d}z = 0. \tag{B20}$$

g. Illustrating $\mathrm{d}^2 = 0$

As illustrated here, the operator relation $\mathrm{d}^2 = 0$ (B12) follows from the commutative property of mixed partial derivatives. Before starting, note that $\mathrm{d}^2 x = \mathrm{d}^2 y = \mathrm{d}^2 z = 0$, which we used in the examples above. These identities result from assuming constant differential increments for each coordinate. That is, as a function, $f(x) = x$ has a constant derivative and thus it has a zero second derivative.

Showing that $\mathrm{d}^2 A = 0$

The 1-form, $\mathrm{d}A$, from equation (B14) has an exterior derivative given by

$$\mathrm{d}^2 A = \mathrm{d}(\partial_x A\,\mathrm{d}x + \partial_y A\,\mathrm{d}y + \partial_z A\,\mathrm{d}z). \tag{B21}$$

Expanding the exterior derivative leads to

$$\begin{aligned} \mathrm{d}^2 A &= (\partial_{yx} A - \partial_{xy} A)\,\mathrm{d}x \wedge \mathrm{d}y \\ &\quad + (\partial_{zy} A - \partial_{yz} A)\,\mathrm{d}y \wedge \mathrm{d}z \\ &\quad + (\partial_{xz} A - \partial_{zx} A)\,\mathrm{d}z \wedge \mathrm{d}x \\ &= 0, \end{aligned} \tag{B22}$$

which follows from equivalence of the mixed partial derivatives.

Showing that $\mathrm{d}^2\mathfrak{A} = 0$

A few lines of algebra reveals that the 2-form, $\mathrm{d}\mathfrak{A}$, from equation (B16), has a vanishing exterior derivative given by

$$\mathrm{d}^2\mathfrak{A} = 0, \tag{B23}$$

which again follows from equality of mixed partial derivatives.

h. Poincaré's Lemma

Consider an arbitrary p-form, φ. We say the φ is closed if it has zero exterior derivative, $\mathrm{d}\varphi = 0$, whereas it is exact if it can be written as the exterior derivative of a $(p\text{-}1)$-form, $\varphi = \mathrm{d}\omega$. Since $\mathrm{d}^2 = 0$, an exact exterior form is also closed:

$$\varphi = \mathrm{d}\omega \implies \mathrm{d}\varphi = \mathrm{d}^2\omega = 0. \tag{B24}$$

Poincaré's Lemma is a statement about the converse: all closed forms on simply connected manifolds are exact

$$\mathrm{d}\varphi = 0 \implies \varphi = \mathrm{d}\omega \tag{B25}$$

for some ω. We made use of this theorem when introducing the water mass configuration space streamfunction in Section 4d.

Equation (B24) generalizes a familiar result from three-dimensional vector analysis, namely that if a vector field $\boldsymbol{v}$ is conservative (it is the gradient of some scalar field f, so that $\boldsymbol{v} = \nabla f$), then it is irrotational (it has zero curl, i.e. $\nabla \times \boldsymbol{v} = \nabla \times \nabla f = 0$). Similarly, equation (B25) generalizes the fact that $\nabla \times \boldsymbol{v} = 0$ implies $\boldsymbol{v} = \nabla f$ for some scalar field f, provided the domain is simply connected.

B5. Stokes-Cartan theorem

The exterior calculus of exterior forms provides an elegant unification of the variety of integral theorems from vector calculus. We refer to the unified integral theorem as the *Stokes-Cartan theorem*, which is written

$$\int_{\mathcal{X}} \mathrm{d}\omega = \int_{\partial\mathcal{X}} \omega. \tag{B26}$$

This relation holds for an exterior form, ω, of arbitrary order and thus for arbitrary dimensional spaces. Furthermore, the manifold $\mathcal{X}$ must be orientable and possess a smooth (or at least a piecewise smooth) boundary. For example, if the space is three-dimensional, then $\mathcal{X}$ is a volume and $\partial\mathcal{X}$ is the surface bounding the volume. If we are instead integrating over a two-dimensional space, then $\mathcal{X}$ is a 2-surface whereas $\partial\mathcal{X}$ is the one-dimensional curve bounding the surface. If we are integrating over a curve, then $\partial\mathcal{X}$ are the endpoints to the curve, in which case the Stokes-Cartan theorem reduces to the fundamental theorem of calculus. Finally, if $\mathcal{X}$ has no boundary, such as the surface of a sphere, then the right hand side of the Stokes-Cartan theorem (B26) vanishes, and so too must the left hand side.

a. The divergence theorem

To connect equation (B26) to the divergence theorem, let $\mathcal{X}$ be a closed volume in 3-space and let $\omega = \mathfrak{B}$, the 2-form given by equation (B2), in which case $\mathrm{d}\omega$ is given by equation (B17b). The Stokes-Cartan theorem (B26) thus specializes to

$$\int_{\mathcal{X}} (\partial_x P + \partial_y Q + \partial_z R)\,\mathrm{d}x \wedge \mathrm{d}y \wedge \mathrm{d}z = \oint_{\partial\mathcal{X}} [P\,\mathrm{d}y \wedge \mathrm{d}z + Q\,\mathrm{d}z \wedge \mathrm{d}x + R\,\mathrm{d}x \wedge \mathrm{d}y]. \quad \text{(B27)}$$

This equation is an expression of the divergence theorem, whereby the volume integral of the divergence of a vector field equals to the vector field integrated over the oriented area of the surface bounding the volume. We emphasize the absence of a surface normal vector, as the exterior products are sufficient to orient the surface integrals.

b. Vector calculus expression of Stokes' theorem

Now set ω equal to the 1-form, $\omega = A\,\mathrm{d}x + B\,\mathrm{d}y + C\,\mathrm{d}z$ as given by equation (B1), so that $\mathrm{d}\omega$ is given by the 2-form in equation (B16). We also compute the integral over a 2-surface, $\mathcal{A}$, with a one-dimensional boundary $\partial\mathcal{A}$. The Stokes-Cartan theorem (B26) is here written

$$\int_{\mathcal{A}} [(\partial_y C - \partial_z B)\,\mathrm{d}y \wedge \mathrm{d}z + (\partial_z A - \partial_x C)\,\mathrm{d}z \wedge \mathrm{d}x + (\partial_x B - \partial_y A)\,\mathrm{d}x \wedge \mathrm{d}y] = \oint_{\partial\mathcal{A}} (A\,\mathrm{d}x + B\,\mathrm{d}y + C\,\mathrm{d}z), \quad \text{(B28)}$$

which is the expression of Stokes' theorem commonly found in vector calculus treatments, where we assumed the right hand rule to orient the closed path integral. On the horizontal plane, with $\mathrm{d}z = 0$, equation (B28) reduces to *Green's Theorem*.

References

Aris, R., 1962: *Vectors, Tensors and the Basic Equations of Fluid Mechanics*. Dover Publishing, New York.

Bi, D., and Coauthors, 2020: Configuration and spin-up of access-cm2, the new generation australian community climate and earth system simulator coupled model. *Journal of Southern Hemisphere Earth Systems Science*, **70 (1)**, 225–251.

Cohen-Tannoudji, C., B. Diu, and F. Laloë, 1977: *Quantum Mechanics: Volume Two*. John Wiley and Sons, New York, 1524 + xxv pp.

Cotter, C. J., and J. Thuburn, 2014: A finite element exterior calculus framework for the rotating shallow-water equations. *Journal of Computational Physics*, **257**, 1506–1526, https://doi.org/10.1016/j.jcp.2013.10.008.

Davis, R. E., 1994: Diapycnal mixing in the ocean: equations for large-scale budgets. *Journal of Physical Oceanography*, **24**, 777–800, https://doi.org/10.1175/1520-0485(1994)024<0777:DMITOE>2.0.CO;2.

Döös, K., J. Kjellson, J. Zika, F. Lalibertè, L. Brodeau, and A. Campino, 2017: The coupled ocean-atmosphere hydrothermohaline circulation. *Journal of Climate*, **30**, 631–647, https://doi.org/10.1175/JCLI-D-15-0759.1.

Döös, K., J. Nilsson, J. Nycander, L. Brodeau, and M. Ballarotta, 2012: The World Ocean thermohaline circulation. *Journal of Physical Oceanography*, **42**, 1445–1460, https://doi.org/10.1175/JPO-D-11-0163.1.

Evans, D. G., J. D. Zika, A. C. Naveira Garabato, and A. G. Nurser, 2014: The imprint of southern ocean overturning on seasonal water mass variability in d rake p assage. *Journal of Geophysical Research: Oceans*, **119 (11)**, 7987–8010.

Evans, D. G., J. D. Zika, A. C. Naveira Garabato, and A. G. Nurser, 2018: The cold transit of southern ocean upwelling. *Geophysical Research Letters*, **45 (24)**, 13–386.

Flanders, H., 1989: *Differential Forms with Applications to the Physical Sciences*. Dover Publications, New York, 224 pp.

Fortney, J., 2018: *A Visual Introduction to Differential Forms and Calculus on Manifolds*. Springer Nature Switzerland, Switzerland, https://doi.org/10.1007/978-3-319-96992-3, 468 pages.

Frankel, T., 2012: *The Geometry of Physics: An Introduction*. Cambridge University Press, 686.

Gill, A., 1982: *Atmosphere-Ocean Dynamics*, International Geophysics Series, Vol. 30. Academic Press, London, 662 + xv pp.

Good, S., M. Martin, and N. A. Rayner, 2013: EN4: Quality controlled ocean temperature and salinity profiles and monthly objective analyses with uncertainty estimates. *Journal of Geophysical Research: Oceans*, **118**, 6704–6716, https://doi.org/10.1002/2013JC009067.

Gregg, M., E. D'Asaro, J. Riley, and E. Kunze, 2018: Mixing efficiency in the ocean. *Annual Reviews of Marine Science*, **10**, 443–473, https://doi.org/10.1146/annurev-marine-121916-063643.

Griffies, S. M., 1998: The Gent-McWilliams skew-flux. *Journal of Physical Oceanography*, **28**, 831–841, https://doi.org/10.1175/1520-0485(1998)028<0831:TGMSF>2.0.CO;2.

Griffies, S. M., 2004: *Fundamentals of Ocean Climate Models*. Princeton University Press, Princeton, USA, 518+xxxiv pages.

Griffies, S. M., A. Adcroft, and R. W. Hallberg, 2020: A primer on the vertical lagrangian-remap method in ocean models based on finite volume generalized vertical coordinates. *Journal of Advances in Modeling Earth Systems*, **12**, https://doi.org/10.1029/2019MS001954.

Groeskamp, S., S. M. Griffies, D. Iudicone, R. Marsh, A. G. Nurser, and J. D. Zika, 2019: The water mass transformation framework for ocean physics and biogeochemistry. *Annual Review of Marine Science*, **11**, 1–35, https://doi.org/10.1146/annurev-marine-010318-095421.

Groeskamp, S., B. M. Sloyan, J. D. Zika, and T. J. McDougall, 2017: Mixing inferred from an ocean climatology and surface fluxes. *Journal of Physical Oceanography*, **47 (3)**, 667–687.

Groeskamp, S., J. D. Zika, T. J. McDougall, B. M. Sloyan, and F. Laliberté, 2014: The representation of ocean circulation and variability in thermodynamic coordinates. *Journal of Physical Oceanography*, **44**, 1735–1750, https://doi.org/10.1175/JPO-D-13-0213.1.

Hieronymus, M., J. Nilsson, and J. Nycander, 2014: Water mass transformation in salinity–temperature space. *Journal of Physical Oceanography*, **44 (9)**, 2547–2568.

Holloway, G., and P. B. Rhines, 1991: Angular momenta of modeled ocean gyres. *Journal of Geophysical Research*, **27**, 843–846, https://doi.org/10.1029/90JC02256.

Holmes, R. M., J. Zika, and M. H. England, 2019: Diathermal heat transport in a global ocean model. *Journal of Physical Oceanography*, **49**, 141–161, https://doi.org/10.1175/JPO-D-18-0098.1.

Iudicone, D., G. Madec, and T. J. McDougall, 2008: Water-mass transformations in a neutral density framework and the key role of light penetration. *Journal of Physical Oceanography*, **38**, 1357–1376, https://doi.org/10.1175/2007JPO3464.1.

Jackett, D. R., and T. J. McDougall, 1997: A neutral density variable for the world's oceans. *Journal of Physical Oceanography*, **27**, 237–263.

Kjellsson, J., K. Döös, F. B. Laliberté, and J. D. Zika, 2014: The atmospheric general circulation in thermodynamical coordinates. *Journal of the Atmospheric Sciences*, **71 (3)**, 916–928.

Laliberté, F., J. D. Zika, L. Mudryk, P. J. Kushner, J. Kjellsson, and K. Döös, 2015: Constrained work output of the moist atmospheric heat engine in a warming climate. *Science*, **347**, 540–543, https://doi.org/10.1126/science.1257103.

Mackay, N., C. Wilson, N. P. Holliday, and J. D. Zika, 2020: The observation-based application of a regional thermohaline inverse method to diagnose the formation and transformation of water masses north of the OSNAP Array from 2013 to 2015. *Journal of Physical Oceanography*, **50**, 1533–1555, https://doi.org/10.1175/JPO-D-19-0188.1.

Mackay, N., C. Wilson, J. D. Zika, and N. P. Holliday, 2018: A regional thermohaline inverse method for estimating circulation and mixing in the Arctic and subpolar North Atlantic. *Journal of Atmospheric and Oceanic Technology*, **35**, 2383–2403, https://doi.org/10.1175/JTECH-D-17-0198.1.

Marshall, J., D. Jamous, and J. Nilsson, 1999: Reconciling thermodynamic and dynamic methods of computation of water-mass transformation rates. *Deep-Sea Research I*, **46**, 545–572, https://doi.org/10.1016/S0967-0637(98)00082-X.

Misner, C. W., K. S. Thorne, and J. A. Wheeler, 1973: *Gravitation*. W.H. Freeman and Co., 1279 pages.

Nurser, A. J. G., R. Marsh, and R. G. Williams, 1999: Diagnosing water mass formation from air–sea fluxes and surface mixing. *Journal of Physical Oceanography*, **29**, 1468–1487, https://doi.org/10.1175/1520-0485(1999)029<1468:DWMFFA>2.0.CO;2.

Olbers, D. J., J. Willebrand, and C. Eden, 2012: *Ocean Dynamics*. 1st ed., Springer, Berlin, Germany, 704 pages.

Pauluis, O. M., and I. M. Held, 2002: Entropy budget of an atmosphere in radiative-convective equilibrium. Part I: Maximum work and frictional dissipation. *Journal of the Atmospheric Sciences*, **59**, 225–139, https://doi.org/10.1175/1520-0469(2002)059<0125:EBOAAI>2.0.CO;2.

Ruan, X., and R. Ferrari, 2021: Diagnosing diapycnal mixing from passive tracers. *Journal of Physical Oceanography*, **51**, 757–767, https://doi.org/10.1175/JPO-D-20-0194.1.

Salmon, R., 1998: *Lectures on Geophysical Fluid Dynamics*. Oxford University Press, Oxford, England, 378 + xiii pp.

Salmon, R., 2013: An alternative view of generalized Lagrangian mean theory. *Journal of Fluid Mechanics*, **719**, 165–182, https://doi.org/10.1017/jfm.2012.638.

Schmitt, R. W., 1994: Double diffusion in oceanography. *Annual Review of Fluid Mechanics*, **26**, 255–285, https://doi.org/10.1146/annurev.fl.26.010194.001351.

Schutz, B. F., 1980: *Geometrical Methods of Mathematical Physics*. Cambridge University Press, Cambridge, UK, 250 pp.

Sohail, T., J. D. Zika, D. B. Irving, and J. A. Church, 2022: Observed poleward freshwater transport since 1970. *Nature*, **602 (7898)**, 617–622.

Speer, K., 1993: Conversion among North Atlantic surface water types. *Tellus*, **45**, 72–79, https://doi.org/10.3402/tellusa.v45i1.14858.

Speer, K., and E. Tziperman, 1992: Rates of water mass formation in the North Atlantic Ocean. *Journal of Physical Oceanography*, **22**, 2444–2457, https://doi.org/10.1175/1520-0485(1992)022<0093:ROWMFI>2.0.CO;2.

Stakgold, I., 2000a: *Boundary value problems of mathematical physics, volume I*. SIAM, Philadelphia, 340 pp.

Stakgold, I., 2000b: *Boundary value problems of mathematical physics, volume II*. SIAM, Philadelphia, 408 pp.

Starr, V. P., 1945: A quasi-Lagrangian system of hydrodynamical equations. *Journal of Meteorology*, **2**, 227–237, https://doi.org/10.1175/1520-0469(1945)002<0227:AQLSOH>2.0.CO;2.

Stommel, H., 1961: Thermohaline convection with two stable regimes of flow. *Tellus*, **13**, 224–228, https://doi.org/10.1111/j.2153-3490.1961.tb00079.x.

van Sebille, E., and Coauthors, 2018: Lagrangian ocean analysis: fundamentals and practices. *Ocean Modelling*, **121**, 49–75, https://doi.org/10.1016/j.ocemod.2017.11.008.

Walin, G., 1977: A theoretical framework for the description of estuaries. *Tellus*, **29 (2)**, 128–136, https://doi.org/10.1111/j.2153-3490.1977.tb00716.x, URL http://dx.doi.org/10.1111/j.2153-3490.1977.tb00716.x.

Walin, G., 1982: On the relation between sea-surface heat flow and thermal circulation in the ocean. *Tellus*, **34**, 187–195, https://doi.org/10.1111/j.2153-3490.1982.tb01806.x.

Warnick, K., R. Selfridge, and D. Arnold, 1997: Teaching electromagnetic field theory using differential forms. *IEEE Transactions on Education*, **40**, 53–68, https://doi.org/10.1109/13.554670.

Warnick, K. F., and P. Russer, 2014: Differential forms and electromagnetic field theory. *Progress In Electromagnetics Research*, **148**, 83–112, https://doi.org/10.2528/PIER14063009.

Weiss, J. B., B. Fox-Kemper, D. Mandal, A. D. Nelson, and R. K. P. Zia, 2019: Nonequilibrium oscillations, probability angular momentum, and the climate system. *Journal of Statistical Physics*, **273–294**, https://doi.org/10.1007/s10955-019-02394-1.

Winters, K. B., and E. A. D'Asaro, 1996: Diascalar flux and the rate of fluid mixing. *Journal of Fluid Mechanics*, **317**, 179–193, https://doi.org/10.1017/S0022112096000717.

Young, W. R., 2012: An exact thickness-weighted average formulation of the Boussinesq equations. *Journal of Physical Oceanography*, **42**, 692–707, https://doi.org/10.1175/JPO-D-11-0102.1.

Zika, J. D., M. H. England, and W. P. Sijp, 2012: The ocean circulation in thermohaline coordinates. *Journal of Physical Oceanography*, **42**, 708–724, https://doi.org/10.1175/JPO-D-11-0139.1.

Zika, J. D., J. M. Gregory, E. L. McDonagh, A. Marzocchi, and L. Clément, 2021: Recent water mass changes reveal mechanisms of ocean warming. *Journal of Climate*, **34**, 3461–3479, https://doi.org/10.1175/JCLI-D-20-0355.1.

Zika, J. D., W. P. Sijp, and M. H. England, 2013: Vertical heat transport by ocean circulation and the role of mechanical and haline forcing. *Journal of physical oceanography*, **43 (10)**, 2095–2112.